

Top eigenvalue of a random matrix: large deviations and third order phase transition

Satya N. Majumdar

Université Paris-Sud, LPTMS, CNRS (UMR 8626), 91405 Orsay Cedex, France

Grégory Schehr

Université Paris-Sud, LPTMS, CNRS (UMR 8626), 91405 Orsay Cedex, France

Abstract. We study the fluctuations of the largest eigenvalue λ_{\max} of $N \times N$ random matrices in the limit of large N . The main focus is on Gaussian β -ensembles, including in particular the Gaussian orthogonal ($\beta = 1$), unitary ($\beta = 2$) and symplectic ($\beta = 4$) ensembles. The probability density function (PDF) of λ_{\max} consists, for large N , of a central part described by Tracy-Widom distributions flanked, on both sides, by two large deviations tails. While the central part characterizes the typical fluctuations of λ_{\max} – of order $\mathcal{O}(N^{-2/3})$ –, the large deviations tails are instead associated to extremely rare fluctuations – of order $\mathcal{O}(1)$. Here we review some recent developments in the theory of these extremely rare events using a Coulomb gas approach. We discuss in particular the third-order phase transition which separates the left tail from the right tail, a transition akin to the so-called Gross-Witten-Wadia phase transition found in 2-d lattice quantum chromodynamics. We also discuss the occurrence of similar third-order transitions in various physical problems, including non-intersecting Brownian motions, conductance fluctuations in mesoscopic physics and entanglement in a bipartite system.

1. Introduction and motivations

Since the pioneering work of Wishart in statistics [1], followed by Wigner and others in nuclear physics [2, 3], Random Matrix Theory (RMT) has found a huge number of applications ranging from statistical physics of disordered systems, mesoscopic physics, quantum information, finance, telecommunication networks to number theory, combinatorics, integrable systems and quantum chromodynamics (QCD), to name just a few [4]. Among the recent developments in RMT, the study of the largest eigenvalue λ_{\max} of large random matrices has attracted particular attention. Questions related to the fluctuations of λ_{\max} belong to the wider topic of extreme value statistics (EVS). Being at the heart of optimization problems, such extreme value questions arise naturally in the statistical physics of complex and disordered systems [5, 6, 7]. In particular, the eigenvalues of a random matrix provide an interesting laboratory to study EVS of *strongly correlated* random variables, and go beyond the three standard universality classes of EVS for independent and identically distributed (i. i. d.) random variables [8].

As realized a long time ago in a seminal paper by May [9], a natural application of the statistics of λ_{\max} is to provide a criterion of physical stability in dynamical systems such as ecosystems. Near a fixed point of a dynamical system, one can linearize the equations of motion and the eigenvalues of the corresponding matrix associated with the linear equations provide important informations about the stability of the fixed point. For example, if all the eigenvalues are negative (or positive) the fixed point is stable (or unstable). As a concrete example, May considered [9] a population of N distinct species with equilibrium densities ρ_i^* , $i = 1, 2, \dots, N$. To start with, they are *noninteracting* and *stable* in the sense that when slightly perturbed from their equilibrium densities, each density relaxes to its equilibrium value with some characteristic damping time. For simplicity, these damping times are all chosen to be unity which sets the time scale. Hence the equations of motion for $x_i(t) = \rho_i(t) - \rho_i^*$, to linear order, are simply $dx_i(t)/dt = -x_i(t)$. Now, imagine switching on pair-wise interactions between the species. May assumed that the interactions between pairs of species can be modeled by a random matrix \mathbf{J} , of size $N \times N$, which is real and symmetric ($J_{ij} = J_{ji}$). The linearized equation of motions close to ρ_i^* then read, in presence of interactions [9]:

$$\frac{dx_i(t)}{dt} = -x_i(t) + \alpha \sum_{j=1}^N J_{ij} x_j(t), \quad (1)$$

where α sets the strength of the interactions. A natural question is then: what is the probability, $P_{\text{stable}}(\alpha, N)$, that the system described by (1) remains stable once the interactions are switched on [9]? In other words, what is the probability that the fixed point $x_i = 0$ for all i remains stable in presence of a nonzero α ? By transforming (1) to the diagonal basis of \mathbf{J} , it is easy to see that the fixed point $x_i = 0$ will remain stable, provided the eigenvalues λ_i of the random matrix \mathbf{J} satisfy the inequality: $\alpha \lambda_i - 1 \leq 0$, for all $i = 1, \dots, N$. This is equivalent to the statement that the largest eigenvalue $\lambda_{\max} = \max_{1 \leq i \leq N} \lambda_i$ satisfies the inequality: $\lambda_{\max} \leq 1/\alpha$. Hence the probability that

the system in (1) is stable gets naturally related to the cumulative distribution function (CDF) of the largest eigenvalue λ_{\max} :

$$P_{\text{stable}}(\alpha, N) = \text{Prob.} [\lambda_{\max} \leq w = 1/\alpha]. \quad (2)$$

Assuming that J_{ij} 's are identical Gaussian random variables with variance $1/N$, i.e. the matrix \mathbf{J} belongs to the Gaussian orthogonal ensemble (GOE) of RMT, May noticed [9] that this cumulative probability (2) undergoes a sharp transition (when $N \rightarrow \infty$) as α increases beyond the critical value $\alpha_c = 1/\sqrt{2}$ (see Fig. 1) [see also [10] for anterior numerical simulations]

$$\lim_{N \rightarrow \infty} P_{\text{stable}}(\alpha, N) = \begin{cases} 1, & \alpha < \alpha_c : \text{stable, weakly interacting phase} \\ 0, & \alpha > \alpha_c : \text{unstable, strongly interacting phase.} \end{cases} \quad (3)$$

May's work was indeed the first direct physical application of the statistics of λ_{\max} and to our knowledge, the first one to point out the existence of a *sharp* phase transition associated with the CDF of λ_{\max} . Several questions follow quite naturally. May's transition occurs strictly in the $N \rightarrow \infty$ limit. What happens for *finite* but large N ? One would expect the sharp transition in Fig. 1 to be replaced by a smooth curve (shown by the dashed lines in Fig. 1), but can one describe analytically the precise form of this curve? Also, is there any *thermodynamical* sense to this stability-instability phase transition? If so, what is the analogue of *free energy* and what is the *order* of this transition? Thanks to the recent developments in RMT on the statistics of λ_{\max} as reviewed in this article, it is possible to answer these questions very precisely. In particular, we will see that the large deviation function of λ_{\max} indeed plays the role of the *free energy* of an underlying Coulomb gas, with a third-order discontinuity exactly at the critical point $\alpha = \alpha_c = 1/\sqrt{2}$, thus rendering it a *third order* phase transition. In addition, this third order phase transition turns out to be rather ubiquitous and occurs in a wide variety of contexts. All these systems share a common mechanism behind this third order phase transition that will be elucidated in this article.

The paper is organized as follows. In section 2, we summarize the main results for the statistics of λ_{\max} for large Gaussian random matrices, with a special focus on the large deviations. In section 3, we describe the Coulomb gas approach which provides a general framework to compute the left and right large deviation tails, which are separated by a third order phase transition. In section 4 we consider various other systems where a similar third order transition occurs and discuss, in some details, three cases namely non-intersecting Brownian motions (and its relation to 2-d quantum chromodynamics), transport through a mesoscopic cavity and the entanglement entropy of a bipartite system in a random pure state. In section 5, we describe the basic mechanism behind this third order phase transition and also discuss its higher order generalizations. Finally we conclude in section 6 with a summary and discussion.

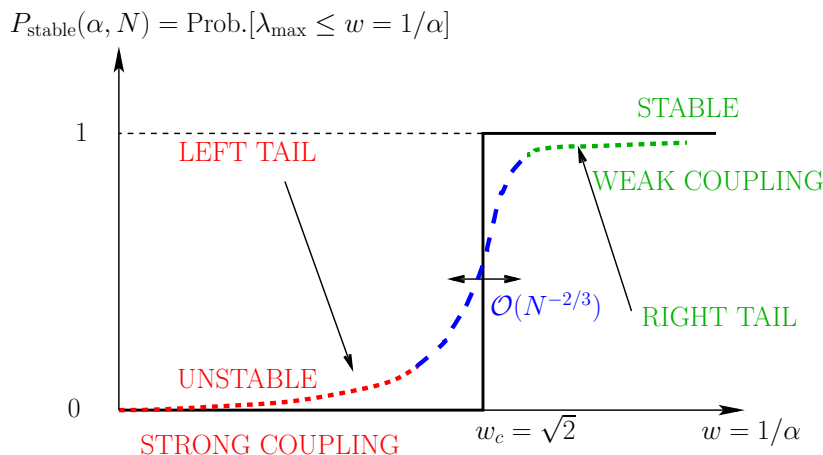


Figure 1. Sketch of the diagram of stability of the system described by (1). The solid line is the limit $N \rightarrow \infty$, illustrating the transition found by May [9] at $w = w_c = \sqrt{2}$. The dashed line corresponds to the large but finite N regime: the central regime (of order $\mathcal{O}(N^{-2/3})$ and described by Tracy-Widom distributions for Gaussian random matrices) is flanked by large deviations tails on both sides. Precise description of the left and the right tail is the main subject of the present article.

2. Main results

We consider $N \times N$ Gaussian random matrices with real symmetric, complex Hermitian, or quaternionic self-dual entries $X_{i,j}$ distributed via the joint law: $\text{Pr}\{\{X_{i,j}\}\} \propto \exp[-c_0 N \text{Tr}(X^2)]$, where c_0 is a constant. This distribution is invariant respectively under orthogonal, unitary and symplectic rotations giving rise to the three classical ensembles: Gaussian orthogonal ensemble (GOE), Gaussian unitary ensemble (GUE) and Gaussian symplectic ensemble (GSE). The eigenvalues and eigenvectors are consequently random and their joint distributions decouple [2, 3]. Integrating out the eigenvectors, we focus here only on the statistics of N eigenvalues $\lambda_1, \lambda_2, \dots, \lambda_N$ which are all real. The joint probability density function (PDF) of these eigenvalues is given by the classical result [2, 3, 11]

$$P_{\text{joint}}(\lambda_1, \lambda_2, \dots, \lambda_N) = B_N \exp \left[-c_0 N \sum_{i=1}^N \lambda_i^2 \right] \prod_{i < j} |\lambda_i - \lambda_j|^\beta, \quad (4)$$

where B_N is a normalization constant and β is called the Dyson index that takes quantized values $\beta = 1$ (GOE), $\beta = 2$ (GUE) and $\beta = 4$ (GSE). For convenience, we choose the constant $c_0 = \beta/2$ and rewrite the statistical weight in (4) as

$$P_{\text{joint}}(\lambda_1, \lambda_2, \dots, \lambda_N) = B_N(\beta) \exp \left[-\beta \left(\frac{N}{2} \sum_{i=1}^N \lambda_i^2 - \frac{1}{2} \sum_{i \neq j} \ln |\lambda_i - \lambda_j| \right) \right]. \quad (5)$$

Hence, this joint law can be interpreted as a Gibbs-Boltzmann measure [12], $P_{\text{joint}}(\{\lambda_i\}) \propto \exp[-\beta E(\{\lambda_i\})]$, of an interacting gas of charged particles on a line where λ_i denotes the position of the i -th charge and β plays the role of the inverse

temperature. The energy $E(\{\lambda_i\})$ has two parts: each pair of charges repel each other via a 2-d Coulomb (logarithmic) repulsion (even though the charges are confined on the 1-d real line) and each charge is subject to an external confining parabolic potential. Note that while $\beta = 1, 2$ and 4 correspond to the three classical rotationally invariant Gaussian ensembles, it is possible to associate a matrix model to (5) for any value of $\beta > 0$ (namely tridiagonal random matrices introduced in [13]). Here we focus on the largest eigenvalue $\lambda_{\max} = \max_{1 \leq i \leq N} \lambda_i$: what can be said about its fluctuations, in particular when N is large? This is a nontrivial question as the interaction term, $\propto |\lambda_i - \lambda_j|^\beta$, renders inapplicable the classical results of extreme value statistics for i. i. d. random variables [8].

The two terms in the energy of the Coulomb gas in (5), the pairwise Coulomb repulsion and the external harmonic potential, compete with each other. While the former tends to spread the charges apart, the later tends to confine the charges near the origin. As a result of this competition, the system of charges settle down into an equilibrium configuration on an average. One can estimate the typical value λ_{typ} of the eigenvalues by balancing the two terms in the energy: the potential energy, which is of order $\sim N^2 \lambda_{\text{typ}}^2$ and the interaction energy, which is of order $\sim N^2$: this yields $\lambda_{\text{typ}} = \mathcal{O}(1)$. The average density of the charges is defined by

$$\rho_N(\lambda) = \frac{1}{N} \left\langle \sum_{i=1}^N \delta(\lambda - \lambda_i) \right\rangle, \quad (6)$$

where the angular brackets denote an average with respect to the joint PDF (5). For such Gaussian matrices (5), it is well known [2, 3, 11] that as $N \rightarrow \infty$, the average density approaches an N -independent limiting form which has a semi-circular shape on the compact support $[-\sqrt{2}, +\sqrt{2}]$

$$\lim_{N \rightarrow \infty} \rho_N(\lambda) = \tilde{\rho}_{\text{sc}}(\lambda) = \frac{1}{\pi} \sqrt{2 - \lambda^2}, \quad (7)$$

where $\tilde{\rho}_{\text{sc}}(\lambda)$ is called the Wigner semi-circular law. Hence it follows from (7) that the average location of λ_{\max} is given by the upper edge of the Wigner semi-circle:

$$\lim_{N \rightarrow \infty} \langle \lambda_{\max} \rangle = \sqrt{2}. \quad (8)$$

From (2, 3), it follows that May's critical point $1/\alpha_c = \sqrt{2}$ (see Fig. 1) coincides precisely with the upper edge of the semi-circle, i.e., with $\langle \lambda_{\max} \rangle = \sqrt{2}$. However, for large but finite N , λ_{\max} will fluctuate from sample to sample and we would like to compute the full CDF of λ_{\max}

$$F_N(w) = \text{Prob.}[\lambda_{\max} \leq w]. \quad (9)$$

From the joint PDF in (5), one can express $F_N(w)$ as a ratio of two partition functions

$$F_N(w) = \frac{Z_N(w)}{Z_N(w \rightarrow \infty)}, \quad (10)$$

$$Z_N(w) = \int_{-\infty}^w d\lambda_1 \cdots \int_{-\infty}^w d\lambda_N \exp \left[-\frac{\beta}{2} \left(N \sum_{i=1}^N \lambda_i^2 - \sum_{i \neq j} \ln |\lambda_i - \lambda_j| \right) \right], \quad (11)$$

where $Z_N(w)$ has a clear physical interpretation: it is the partition function of a 2-d Coulomb gas, confined on a 1-d line and subject to a harmonic potential, in presence of a *hard wall* at w [14]. The study of this ratio of two partition functions (10) reveals the existence of two distinct scales corresponding to (i) typical fluctuations of the top eigenvalue, where $\lambda_{\max} = \mathcal{O}(N^{-2/3})$ and (ii) atypical large fluctuations where $\lambda_{\max} = \mathcal{O}(1)$: these two cases need to be studied separately.

2.1. Typical fluctuations

To estimate the typical scale $\delta\lambda_{\max}$ of the fluctuations of λ_{\max} , going beyond the estimate in (8), one can apply the standard criterion of EVS, i.e.

$$\int_{\sqrt{2}-\delta\lambda_{\max}}^{\sqrt{2}} \tilde{\rho}_{\text{sc}}(\lambda) d\lambda \sim \frac{1}{N}, \quad (12)$$

which simply says that the fraction of eigenvalues to the right of the maximum (including itself) is typically $1/N$. Using the asymptotic behavior near the upper edge (7), $\rho_{\text{sc}}(\lambda) \propto (\sqrt{2} - \lambda)^{1/2}$ as $\lambda \rightarrow \sqrt{2}$, one obtains [15, 16]

$$\delta\lambda_{\max} = \sqrt{2} - \lambda_{\max} = \mathcal{O}(N^{-2/3}). \quad (13)$$

More precisely, it turns out that as $N \rightarrow \infty$

$$\lambda_{\max} = \sqrt{2} + \frac{1}{\sqrt{2}} N^{-2/3} \chi_{\beta}, \quad (14)$$

where χ_{β} is an N -independent random variable. Its CDF, $\mathcal{F}_{\beta}(x) = \text{Prob}[\chi_{\beta} \leq x]$, is known as the β -Tracy-Widom (TW) distribution which is known explicitly only for $\beta = 1, 2$ and 4 . Tracy and Widom indeed obtained an explicit expression for $\beta = 2$ first [17] and subsequently for $\beta = 1$ and 4 [18] in terms of the Hastings-McLeod solution of the Painlevé II equation

$$q''(s) = 2q^3(s) + sq(s), \quad q(s) \sim \text{Ai}(s), \quad s \rightarrow \infty. \quad (15)$$

The CDF $\mathcal{F}_{\beta}(x)$ is then given explicitly for $\beta = 1, 2$ and 4 by [17, 18]

$$\begin{aligned} \mathcal{F}_1(x) &= \exp \left[-\frac{1}{2} \int_x^{\infty} [(s-x)q^2(s) + q(s)] ds \right], \\ \mathcal{F}_2(x) &= \exp \left[-\int_x^{\infty} (s-x)q^2(s) ds \right], \\ \mathcal{F}_4(2^{-\frac{2}{3}}x) &= \exp \left[-\frac{1}{2} \int_x^{\infty} (s-x)q^2(s) ds \right] \cosh \left[\frac{1}{2} \int_x^{\infty} q(s) ds \right]. \end{aligned} \quad (16)$$

For other values of β it can be shown that χ_{β} describes the fluctuations of the ground state of the following one-dimensional Schrödinger operator, called the “stochastic Airy operator” [19, 20]

$$\mathcal{H}_{\beta} = -\frac{d^2}{dx^2} + x + \frac{2}{\sqrt{\beta}}\eta(x), \quad (17)$$

where $\eta(x)$ is Gaussian white noise, of zero mean and with delta correlations, $\overline{\eta(x)\eta(x')} = \delta(x - x')$. For arbitrary $\beta > 0$, the CDF $\mathcal{F}_\beta(x)$, or equivalently the PDF $\mathcal{F}'_\beta(x)$ of χ_β has rather asymmetric non-Gaussian tails,

$$\mathcal{F}'_\beta(x) \approx \begin{cases} \exp\left[-\frac{\beta}{24}|x|^3\right], & x \rightarrow -\infty \\ \exp\left[-\frac{2\beta}{3}x^{3/2}\right], & x \rightarrow +\infty, \end{cases} \quad (18)$$

where \approx stands for a logarithmic equivalent [see below for more precise asymptotics (49, 55)]. These TW distributions also describe the top eigenvalue statistics of large real [21, 22] and complex [23] Gaussian Wishart matrices. Amazingly, the same TW distributions have emerged in a number of a priori unrelated problems [24] such as the longest increasing subsequence of random permutations [25], directed polymers [23, 26] and growth models [27] in the Kardar-Parisi-Zhang (KPZ) universality class in (1 + 1) dimensions as well as for the continuum (1+1)-dimensional KPZ equation [28, 29, 30, 31], sequence alignment problems [32], mesoscopic fluctuations in quantum dots [33], height fluctuations of non-intersecting Brownian motions over a fixed time interval [34, 35], height fluctuations of non-intersecting interfaces in presence of a long-range interaction induced by a substrate [36], and also in finance [37]. Remarkably, the TW distributions have been recently observed in experiments on nematic liquid crystals [38] (for $\beta = 1, 2$) and in experiments involving coupled fiber lasers [39] (for $\beta = 1$).

2.2. Atypical fluctuations and large deviations

While the TW density describes the probability of *typical* fluctuations of λ_{\max} around its mean $\langle \lambda_{\max} \rangle = \sqrt{2}$ on a *small* scale of $\sim \mathcal{O}(N^{-2/3})$, it does not describe *atypically* large fluctuations, e.g. of order $\mathcal{O}(1)$ around its mean. Questions related to large deviations of extreme eigenvalues have recently emerged in a variety of contexts including cosmology [40, 41, 42], disordered systems such as spin glasses [14, 43, 44, 45, 46, 47], and in the assessment of the efficiency of data compression [48]. The probability of atypically large fluctuations, to leading order for large N , is described by two large deviations (or rate) functions $\Phi_-(x)$ (for fluctuations to the *left* of the mean) and $\Phi_+(x)$ (for fluctuations to the *right* of the mean). More precisely, the behavior of the CDF $F_N(w)$ of λ_{\max} for large but finite N (as depicted schematically by the dashed lines in Fig. 1) is described as follows

$$F_N(w) \approx \begin{cases} \exp[-\beta N^2 \Phi_-(w)] & , w < \sqrt{2} \ \& \ |w - \sqrt{2}| \sim \mathcal{O}(1) \\ \mathcal{F}_\beta\left(\sqrt{2}N^{\frac{2}{3}}(w - \sqrt{2})\right) & , |w - \sqrt{2}| \sim \mathcal{O}(N^{-\frac{2}{3}}) \\ 1 - \exp[-\beta N \Phi_+(w)] & , w > \sqrt{2} \ \& \ |w - \sqrt{2}| \sim \mathcal{O}(1). \end{cases} \quad (19)$$

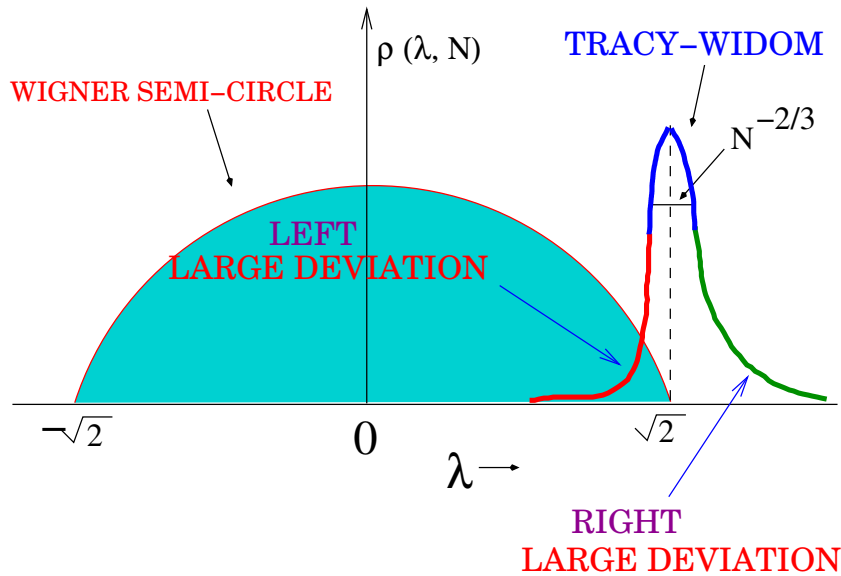


Figure 2. Sketch of the pdf of λ_{\max} with a peak around the right edge of the Wigner semicircle $\langle \lambda_{\max} \rangle = \sqrt{2}$. The typical fluctuations of order $\mathcal{O}(N^{-2/3})$ around the mean are described by the Tracy-Widom density (blue), while the large deviations of order $\mathcal{O}(1)$ to the left and right of the mean $\langle \lambda_{\max} \rangle = \sqrt{2}$ are described by the left (red) and right (green) large deviation tails.

Equivalently, the PDF of λ_{\max} , obtained from the derivative $dF_N(w)/dw$ reads (keeping only leading order terms for large N)

$$\mathcal{P}(\lambda_{\max} = w, N) \approx \begin{cases} \exp[-\beta N^2 \Phi_-(w)] & , w < \sqrt{2} \text{ \& } |w - \sqrt{2}| \sim \mathcal{O}(1) \\ \sqrt{2} N^{\frac{2}{3}} \mathcal{F}'_{\beta} \left(\sqrt{2} N^{\frac{2}{3}} (w - \sqrt{2}) \right) & , |w - \sqrt{2}| \sim \mathcal{O}(N^{-\frac{2}{3}}) \\ \exp[-\beta N \Phi_+(w)] & , w > \sqrt{2} \text{ \& } |w - \sqrt{2}| \sim \mathcal{O}(1) . \end{cases} \quad (20)$$

A schematic picture of this probability density is shown in Fig. 2. We will see later that the physical mechanism responsible for the left tail (*pushed* Coulomb gas) is very different from the one on the right (*pulled* Coulomb gas).

Note that while the TW distribution $\mathcal{F}_{\beta}(x)$, describing the central part of the probability distribution of λ_{\max} , depends explicitly on β [see Eq. (16)], the two leading order rate functions $\Phi_{\mp}(w)$ are independent of β . Exploiting a simple physical method based on the Coulomb gas (see below), the left rate function $\Phi_-(z)$ was first explicitly computed in [14, 45]

$$\Phi_-(w) = \frac{1}{108} \left[36w^2 - w^4 - (15w + w^3) \sqrt{w^2 + 6} + 27 \left(\ln 18 - 2 \ln \left(w + \sqrt{w^2 + 6} \right) \right) \right] , w < \sqrt{2} . \quad (21)$$

Note in particular the behavior when w approaches the critical point from below:

$$\Phi_-(w) \sim \frac{1}{6\sqrt{2}}(\sqrt{2} - w)^3, \quad w \rightarrow \sqrt{2}. \quad (22)$$

On the other hand, the right rate function $\Phi_+(w)$ was computed in [48]. A more complicated, albeit mathematically rigorous, derivation (but only valid for $\beta = 1$) of $\Phi_+(w)$ in the context of spin glass models can be found in [49]. Incidentally, the right tail of λ_{\max} can also be directly related to the finite N behavior of the average density of states to the right of the Wigner sea [50]. Indeed, for $\beta = 1$, this finite N right tail of the density was computed in Ref. [51], from which one can extract the right rate function $\Phi_+(w)$. It reads

$$\Phi_+(w) = \frac{1}{2}w\sqrt{w^2 - 2} + \ln \left[\frac{w - \sqrt{w^2 - 2}}{\sqrt{2}} \right], \quad (23)$$

with the asymptotic behavior

$$\Phi_+(w) \sim \frac{2^{7/4}}{3}(w - \sqrt{2})^{3/2}, \quad w \rightarrow \sqrt{2}. \quad (24)$$

More recently, the sub-leading corrections to the leading behavior have been explicitly computed using more sophisticated methods both for the left tail [52], as well as for the right tail [53, 54, 55] [see also Eqs. (48, 54) below]. It is interesting to note that these explicit expressions for the rate functions $\Phi_{\pm}(z)$ [respectively in Eqs. (23) and (21)] have been used recently to compute exactly the complexity of a class of spin glass models [46, 47]. Finally, we mention that a one-parameter extension of the rate function $\Phi_+(w)$ in (23) was found in Ref. [56] in the context of the statistics of the global maximum of random quadratic forms over a sphere.

2.3. Third order phase transition and matching

The different behavior of $\mathcal{P}(\lambda_{\max} = w, N) = F'_N(w)$ in (20) for $w < \sqrt{2}$ and $w > \sqrt{2}$ leads, in the limit $N \rightarrow \infty$, to a phase transition at the critical point $w_c = \sqrt{2}$. This is exactly the transition found by May in (3), with $\alpha_c = 1/w_c = 1/\sqrt{2}$ (see Fig. 1). Here one can give a physical meaning to this transition as it corresponds to a thermodynamical phase transition for the free energy, $\propto \ln F_N(w)$, of a Coulomb gas, in presence of a wall (10) as the position of the wall w crosses the critical value w_c . One has indeed, from (19):

$$\lim_{N \rightarrow \infty} -\frac{1}{N^2} \ln F_N(w) = \begin{cases} \Phi_-(w), & w < \sqrt{2}, \\ 0 & w > \sqrt{2}, \end{cases} \quad (25)$$

where $\Phi_-(w)$ is given in (21). Since $\Phi_-(w) \sim (\sqrt{2} - w)^3$ when w approaches $\sqrt{2}$ from below (22), the third derivative of the free energy of the Coulomb gas at the critical point $w_c = \sqrt{2}$ is discontinuous: this can thus be interpreted as a *third order phase transition*.

This third order phase transition is very similar to the so called Gross-Witten-Wadia phase transition which was found in the 80's in the context of two-dimensional $U(N)$ lattice quantum chromodynamics (QCD) [57, 58]. It was indeed shown in [57, 58]

that the partition function Z of the $U(N)$ lattice QCD in two dimensions with Wilson's action can be reduced to $Z = \zeta^{N_p}$, where N_p is the number of plaquettes in 2-d and $\zeta = \int \mathcal{D}U \exp [(N/g) \text{Tr} (U + U^\dagger)]$ is a single matrix integral. Here U is an $N \times N$ unitary matrix drawn from the uniform Haar measure and g is the coupling strength. By analyzing ζ in the large N limit, it was shown that the free energy per plaquette $\lim_{N \rightarrow \infty} -(1/N^2) \ln \zeta$ undergoes a third order phase transition at a critical coupling strength $g_c = 2$ separating a strong coupling phase ($g > g_c = 2$) and a weak coupling phase ($g < g_c = 2$). In this case, because the matrix U is unitary, its eigenvalues λ_j 's lie on the unit circle and are parameterized by angles θ_j 's, with $\lambda_j = e^{i\theta_j}$. The average density of eigenvalues, in the limit $N \rightarrow \infty$, is given explicitly by [57, 58]

$$\rho^*(\theta) = \begin{cases} \frac{2}{\pi g} \cos \left[\frac{\theta}{2} \sqrt{\frac{g}{2} - \sin^2 \left(\frac{\theta}{2} \right)} \right], & 0 \leq |\theta| \leq 2 \sin^{-1} \left(\sqrt{\frac{g}{2}} \right), \text{ for } g \leq 2 \\ \frac{1}{2\pi} \left(1 + \frac{2}{g} \cos \theta \right), & \theta \in [-\pi, +\pi], \text{ for } g \geq 2. \end{cases} \quad (26)$$

When $g < 2$, the eigenvalues are thus confined on an arc of the circle $-2 \sin^{-1} \left(\sqrt{\frac{g}{2}} \right) \leq \theta \leq 2 \sin^{-1} \left(\sqrt{\frac{g}{2}} \right)$. As $g \rightarrow 2$ from below, the charge density covers the full circle. Hence in this case the limiting angles $\pm\pi$ play the role of hard walls for the eigenvalues and the gap between the edges of the arc and the hard wall $\pm\pi$ vanishes exactly as g approaches the critical point $g = 2$ from below. For $g > 2$, the density at the hard wall $\pm\pi$ has a nonzero finite value [see (26)].

This third order transition from the strong to the weak coupling phase turns out to be similar to the third order stable-unstable transition in May's model as described in (25) (see also Fig. 1). Indeed, to bring out the similarities between the two models one can draw their respective phase diagrams as in Fig. 3. Thus, the weak (strong) coupling phase in the $U(N)$ QCD is the analogue of the stable (unstable) phase in May's model. In Fig. 3, strictly in the $N \rightarrow \infty$ limit, one has a sharp phase transition in both models as one goes through the critical point on the horizontal axis. However, for finite but large N , this sharp phase transition gets rounded off and the 'critical point' gets splayed out into a *critical crossover zone*. As one increases g or α , the system crosses over from the weak coupling (stable) to the strong coupling (unstable) phase over this critical zone. In May's model (right panel of Fig. 3), while the large deviation functions in (20) describe the free energy deep inside the two phases (stable and unstable), the Tracy-Widom distribution describes precisely the crossover behavior of the free energy from one phase to the other as one traverses the *critical zone* at finite N . Later we will come back to a related third order transition, the so-called Douglas-Kazakov transition [59], found for continuum two dimensional QCD (see Fig. 7 below).

To investigate how smoothly this *crossover* occurs, it is interesting to match the central Tracy-Widom regime (around the peak) in Fig. 2 with the two far tails

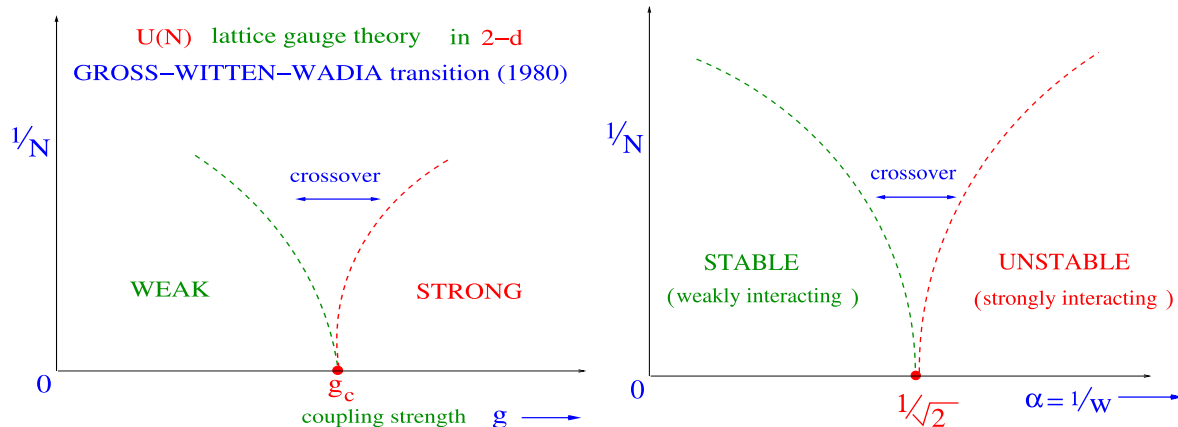


Figure 3. Phase diagrams of the $U(N)$ lattice QCD model where g is the coupling strength (left panel) and the May's dynamical system with α denoting the interaction strength between species (right panel).

characterized by the rate functions in (22) and (24). Indeed, one can check that the expansion of the large deviation functions around the critical point $w_c = \sqrt{2}$ matches smoothly with the asymptotic tails of the β -Tracy-Widom scaling function in the central region. To see this, let us first consider the left tail in (20), i.e. when $w < \sqrt{2}$. When $w \rightarrow \sqrt{2}$ from below we can substitute the asymptotic behavior of the rate function $\Phi_-(w)$ from (22) in the first line of (20). This yields for $1 \ll \sqrt{2} - w \ll \sqrt{2}$

$$\mathcal{P}(\lambda_{\max} = w, N) = \frac{d}{dw} F_N(w) \approx \exp\left(-\frac{\beta}{6\sqrt{2}} N^2 (\sqrt{2} - w)^3\right). \quad (27)$$

On the other hand, consider now the second line of (20) that describes the central typical fluctuations. When the deviation from the typical value $w_c = \sqrt{2}$ is large ($\sqrt{2} - w \sim \mathcal{O}(1)$) we can substitute in the second line of (20) the left tail asymptotic behavior of the β -Tracy-Widom distribution (18) giving

$$\mathcal{P}(\lambda_{\max} = w, N) = \frac{d}{dw} F_N(w) \approx \exp\left[-\frac{\beta}{24} \left[2^{1/2} N^{2/3} (\sqrt{2} - w)\right]^3\right], \quad (28)$$

which after a trivial rearrangement, is identical to (27). This shows that the left tail of the central region matches smoothly with the left large deviation function. Similarly, on the right side, using the behavior of $\Phi_+(x)$ in (24), one finds from (20) that

$$\mathcal{P}(\lambda_{\max} = w, N) = \frac{d}{dw} F_N(w) \approx \exp\left(-\frac{2^{7/4}\beta}{3} N (w - \sqrt{2})^{3/2}\right), \quad (29)$$

for $1 \ll w - \sqrt{2} \ll \sqrt{2}$, which matches with the right tail of the central part described by $\mathcal{F}'_\beta(x)$ (18). Such a mechanism of matching between the central part and the large deviation tails of the distribution have been found in other similar problems [48, 60] (see also Ref. [61] for a counterexample) that will be discussed later.

So far we have mainly focused on the Gaussian β -ensembles of random matrices, whose eigenvalues are distributed via (5). Other interesting ensembles of RMT include

the Wishart random matrices [1] (also called the Laguerre ensemble of RMT), which play an important role in Principal Component Analysis of large datasets. A Wishart matrix \mathbf{W} can be viewed as a correlation matrix, built from the product $\mathbf{W} = \mathbf{X}^\dagger \mathbf{X}$ where \mathbf{X} is a $M \times N$ random Gaussian matrix (real or complex). The joint PDF of the eigenvalues reads in this case [62]

$$P_{\text{joint}}^W(\lambda_1, \dots, \lambda_N) = B_N^W(\beta, \gamma_0) \left(\prod_{i=1}^N \lambda_i^{\gamma_0 \beta / 2} \right) \Delta_N^\beta(\lambda_1, \dots, \lambda_N) e^{-\frac{N\beta}{2} \sum_{i=1}^N \lambda_i}, \quad (30)$$

where

$$\Delta_N(\lambda_1, \dots, \lambda_N) = \prod_{1 \leq i < j \leq N} (\lambda_i - \lambda_j) \quad (31)$$

is the Vandermonde determinant and $\gamma_0 = (1 + M - N) - 2/\beta$ and $B_N^W(\beta, \gamma_0)$ is a normalization constant. In this case, the Wigner semi-circle law (7) for the average density of eigenvalues is replaced by the Marčenko-Pastur distribution [63]. For $M \geq N$ and setting $c = N/M \leq 1$, the Marčenko-Pastur density has a compact support $[a, b]$ where $a = (c^{-1/2} - 1)^2$ and $b = (c^{-1/2} + 1)^2$ and is given explicitly by

$$\lim_{N \rightarrow \infty} \frac{1}{N} \sum_{i=1}^N \langle \delta(\lambda - \lambda_i) \rangle = \tilde{\rho}_{\text{MP}}(\lambda) = \frac{1}{2\pi\lambda} \sqrt{(\lambda - a)(b - \lambda)}. \quad (32)$$

Note that, like the Wigner semi-circle law (7), $\tilde{\rho}_{\text{MP}}(\lambda)$ vanishes like $\propto \sqrt{b - \lambda}$ near the right edge of the support. From (32) one deduces that $\lim_{N \rightarrow \infty} \langle \lambda_{\text{max}} \rangle = b$. While the typical fluctuations of λ_{max} , which are of order $\mathcal{O}(N^{-2/3})$, are also given by TW distributions [21, 22, 23], the large deviations exhibit a behavior similar to, albeit different from (20):

$$\mathcal{P}(\lambda_{\text{max}} = w, N) \approx \begin{cases} \exp[-\beta N^2 \Psi_-(w)], & w < b \ \& \ |w - b| \sim \mathcal{O}(1), \\ \exp[-\beta N \Psi_+(w)], & w > b \ \& \ |w - b| \sim \mathcal{O}(1), \end{cases} \quad (33)$$

where the rate functions $\Psi_-(w)$ and $\Psi_+(w)$ have been computed exactly respectively in Ref. [60] and Ref. [48] (and are different from $\Phi_+(w)$ and $\Phi_-(w)$ found for Gaussian random matrices). Here also, using the behavior of $\Psi_-(w)$ when w approaches the critical value b from below, one can show that the CDF of λ_{max} also exhibits a third order phase transition, similar to the one found for Gaussian β -ensembles (25). Remarkably, both large deviation functions $\Psi_-(w)$ and $\Psi_+(w)$ have been measured in experiments involving coupled fiber lasers [39]. We note that large deviation functions associated with the minimum eigenvalue at the left edge of the Marčenko-Pastur sea (for $c < 1$ strictly) have also been studied by similar Coulomb gas method [64, 65]. For $c = 1$ (the hard edge case where $M - N \ll \mathcal{O}(N)$ for large N), the minimum eigenvalue distribution has also been studied extensively [16, 66, 67] (for a recent review see Ref. [68]), with very nice applications in QCD [69] and in bipartite quantum systems in a random pure state [70]. Large deviations functions of λ_{max} for spiked Wishart ensembles were also

computed in Ref. [71]. Finally, we point out that the large deviation functions associated with Cauchy ensembles of random matrices have recently been computed exactly using a similar Coulomb gas method [72].

3. Derivation of large deviation tails using Coulomb gas method

In this section we briefly summarize the Coulomb gas method that allows us to extract the large N behavior of $F_N(w) = \text{Prob.}[\lambda_{\max} \leq w]$. We first express $F_N(w)$ as a ratio of two partition functions as in (10) where $Z_N(w)$ is expressed as a multiple N -fold integral with a fixed upper bound at w

$$Z_N(w) = \int_{-\infty}^w d\lambda_1 \cdots \int_{-\infty}^w d\lambda_N \exp[-\beta N^2 E[\{\lambda_i\}]] \quad (34)$$

$$E[\{\lambda_i\}] = \frac{1}{2N} \sum_{i=1}^N \lambda_i^2 - \frac{1}{2N^2} \sum_{j \neq k} \log |\lambda_j - \lambda_k|. \quad (35)$$

The main idea then is to evaluate this multiple integral for large N , but with a fixed w , via the steepest descent (saddle point) method. When N is large, the Coulomb gas with N discrete charges can be characterized by a continuous charge density

$$\rho_w(\lambda) = \frac{1}{N} \sum_{i=1}^N \delta(\lambda - \lambda_i), \quad (36)$$

such that $\rho_w(\lambda)d\lambda$ counts the fraction of eigenvalues between λ and $\lambda + d\lambda$. It is normalized to unity and, because of the presence of the wall, one has obviously $\rho_w(\lambda) = 0$ for $\lambda > w$. The next step is then to replace the multiple integral in (34) by a functional integral over the space of all possible normalized densities $\rho_w(\lambda)$. This gives [14, 45]

$$Z_N(w) \propto \int \mathcal{D}[\rho_w] \exp[-\beta N^2 \mathcal{E}[\rho_w] + \mathcal{O}(N)] \delta\left(\int_{-\infty}^w \rho_w(\lambda) d\lambda - 1\right), \quad (37)$$

$$\mathcal{E}[\rho_w] = \frac{1}{2} \int_{-\infty}^w \lambda^2 \rho_w(\lambda) - \frac{1}{2} \int_{-\infty}^w d\lambda \int_{-\infty}^w d\lambda' \rho_w(\lambda) \rho_w(\lambda') \ln(|\lambda - \lambda'|), \quad (38)$$

where the terms of order $\mathcal{O}(N)$ in the exponent in (37) come from the entropy term associated with the density field ρ_w when going from the multiple N -fold integral to a functional integral [12]. Roughly speaking, it corresponds to all microscopic charge configurations compatible with a given macroscopic density $\rho_w(\lambda)$. This entropic contribution was explicitly computed recently for Gaussian ensembles in Ref. [73] and for the Wishart-Laguerre ensembles in Ref. [74]. But here, we will mainly be concerned with the leading energy term $\sim \mathcal{O}(N^2)$ and hence will ignore the entropy term.

We next evaluate the functional integral in the large N limit using the saddle point method. The density at the saddle point $\rho_w^*(\lambda)$ minimizes the energy $\mathcal{E}[\rho_w]$ subject to the constraint $\int_{-\infty}^w \rho_w^*(\lambda) d\lambda = 1$. Hence $\rho_w^*(\lambda)$ is a stationary point of the following action $S[\rho_w(\lambda)]$

$$\left. \frac{\delta S[\rho_w]}{\delta \rho_w} \right|_{\rho_w = \rho_w^*} = 0, \quad S[\rho_w] = \mathcal{E}[\rho_w] + C \left(\int_{-\infty}^w \rho_w(\lambda) d\lambda - 1 \right), \quad (39)$$

where C is a Lagrange multiplier that ensures the normalization condition of the density. Another alternative way to arrive at the same result is to replace the delta function in (37) by its integral representation and then minimize the resulting action. Once the saddle point density $\rho_w^*(\lambda)$ is found from (39), one can compute the CDF of λ_{\max} from (10, 37) as

$$F_N(w) \approx \exp \left[-\beta N^2 (\mathcal{E}[\rho_w^*] - \mathcal{E}[\rho_\infty^*]) \right], \quad (40)$$

where $\rho_\infty^*(\lambda) = \lim_{w \rightarrow \infty} \rho_w^*(\lambda)$. Thus we see that the cumulative distribution of λ_{\max} (which is a probabilistic quantity) can be interpreted thermodynamically. Its logarithm can be expressed as the free energy difference between two Coulomb gases: one in presence of a hard wall at w and the other is free, i.e., the wall is located at infinity.

The next step is thus to determine the solution of the saddle point equation (39). Setting the functional derivative to zero in (39) gives the following integral equation

$$\frac{\lambda^2}{2} - \int \rho_w^*(\lambda') \ln(|\lambda - \lambda'|) d\lambda' + C = 0, \quad (41)$$

which is valid only over the support of $\rho_w^*(\lambda)$, i.e, where this density is nonzero. Clearly, the solution can not have an unbounded support. Because, if that was so, for large λ , the first term in (41) grows as λ^2 whereas the second term grows as $\ln(|\lambda|)$ and hence they can never balance each other. Evidently, then the solution must have a finite support over $[a_1, a_2]$ and assuming that this is a single compact support, the range of integration in (41) can be set from a_1 to a_2 (with $a_2 > a_1$). Deriving once again (41) with respect to λ (and for $\lambda \in [a_1, a_2]$), we can get rid of the constant C and get a singular Cauchy type equation

$$\lambda = \mathcal{f}_{a_1}^{a_2} \frac{\rho_w^*(\lambda')}{\lambda - \lambda'}, d\lambda' \quad (42)$$

where \mathcal{f} denotes the principal value of the integral. Eq. (42) belongs to the general class of Cauchy singular integral equations (with one compact support) of the form

$$g(\lambda) = \mathcal{f}_{a_1}^{a_2} \frac{\rho(\lambda')}{\lambda - \lambda'} d\lambda', \quad (43)$$

valid over the single support $\lambda \in [a_1, a_2]$ and with an arbitrary source function $g(\lambda)$. The problem is to invert this equation, i.e., find $\rho(\lambda)$ given $g(\lambda)$. Fortunately, such singular integral equations can be explicitly inverted using a formula due to Tricomi [75] that reads

$$\rho(\lambda) = \frac{1}{\pi \sqrt{(a_2 - \lambda)(\lambda - a_1)}} \left[C_0 - \mathcal{f}_{a_1}^{a_2} \frac{dt \sqrt{(a_2 - t)(t - a_1)}}{\pi (\lambda - t)} g(t) \right] \quad (44)$$

where $C_0 = \int_{a_1}^{a_2} \rho(\lambda) d\lambda$ is a constant. In our case, the source function $g(\lambda) = \lambda$ and the constant $C_0 = 1$ due to the normalization $\int_{a_1}^{a_2} \rho_w(\lambda) d\lambda = 1$. Fortunately, the principal value of the integral in (44) with $g(t) = t$ can be explicitly computed. The unknown edges a_1 and a_2 can also be completely determined leading to the following

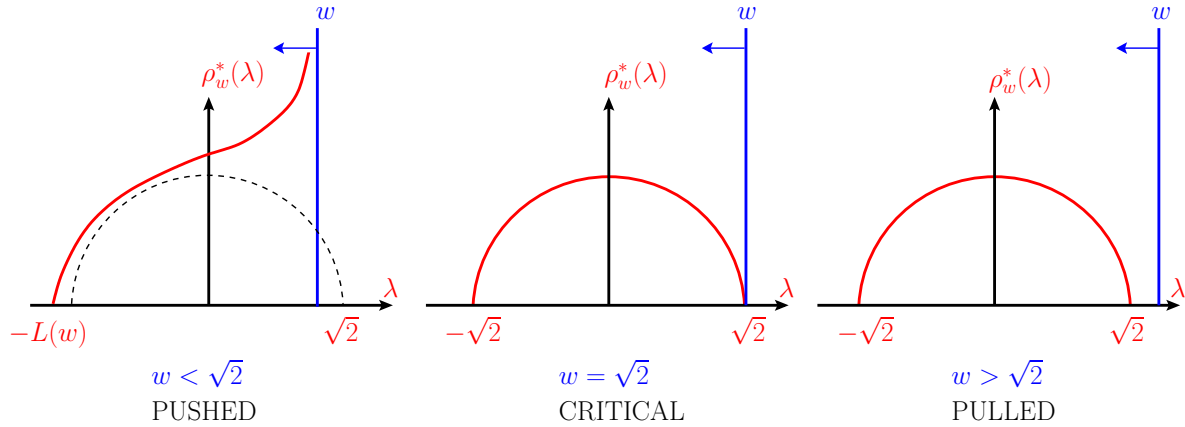


Figure 4. Effect of the presence of a wall on the Wigner semi-circle. If $w < \sqrt{2}$, the density is *pushed* which leads to a complete reorganization of the density charges will if $w > \sqrt{2}$ a single charge is *pulled*, leaving the bulk of the density unchanged.

exact result [14, 45]

$$\rho_w^*(\lambda) = \begin{cases} \frac{1}{\pi} \sqrt{2 - \lambda^2}, & \text{with } -\sqrt{2} \leq \lambda \leq \sqrt{2} & \text{for } w > \sqrt{2} \\ \frac{\sqrt{\lambda + L(w)}}{2\pi\sqrt{w - \lambda}} [w + L(w) - 2\lambda] & \text{with } -L(w) \leq \lambda \leq w & \text{for } w < \sqrt{2} \end{cases} \quad (45)$$

where

$$L(w) = \frac{2\sqrt{w^2 + 6} - w}{3}. \quad (46)$$

Note in particular that, in presence of a pushing wall ($w < \sqrt{2}$), the density diverges close to the wall, $\rho_w^*(\lambda) \propto 1/\sqrt{w - \lambda}$ as $\lambda \rightarrow w$.

Thus, to leading order for large N , the saddle density sticks to the Wigner semi-circular form as long as $w > w_c = \sqrt{2}$, but changes its form when $w < w_c = \sqrt{2}$ (see Fig. 4). This solution makes complete physical sense. Consider first the limit $w \rightarrow \infty$. In this case, the equilibrium charge density of the Coulomb gas is evidently of the Wigner semi-circular form. Now, imagine bringing the wall from infinity closer to the origin. As long as the wall position is bigger than the right edge $\sqrt{2}$ of the semi-circle, the charges do not feel the existence of the wall and are happy to equilibrate into the semi-circular form, thus giving rise to the solution in (45) for $w > \sqrt{2}$. When the wall position w hits the edge of the semi-circle, i.e., when $w \rightarrow \sqrt{2}$ from above, the charges start feeling the wall and finally when $w < \sqrt{2}$, i.e., the charge density gets *pushed* by the wall, the charges have to re-organize to find a new equilibrium density that minimizes the energy, leading to the new deformed solution in (45). This is indeed the mechanism behind the phase transition, driven by the vanishing of the the gap between the wall and the edge of the Coulomb gas droplet.

Finally, injecting the saddle point solution into the action in (40), one then gets,

to leading order for large N , the result announced in (25)

$$F_N(w) \approx \begin{cases} \exp[-\beta N^2 \Phi_-(w)] & \text{for } w < \sqrt{2}, \\ 1 & \text{for } w > \sqrt{2}, \end{cases} \quad (47)$$

where $\Phi_-(w)$ is given explicitly in (21). Note that the complete re-organization of the charge density for $w < w_c$ costs an energy of order $\sim \mathcal{O}(N^2)$, and $\Phi_-(w)$ is proportional to this energy cost. The left rate function $\Phi_-(w)$ vanishes as $\sim (\sqrt{2} - w)^3$ as w approaches to the critical point $\sqrt{2}$ from below, thus making the transition third order.

As an aside, we note that recently the higher order corrections for the left tail were computed in [52] using a method based on the so called loop-equations and their large N expansion [76]. It was shown that

$$-\ln[\mathcal{P}(\lambda_{\max} = w, N)] = N^2 \Phi_+(w) + N(\beta - 2)\Psi_1(w) + (\ln N)\phi_\beta(w) + \Psi_2(\beta, w) + \mathcal{O}(1/N), \quad (48)$$

where the functions Ψ_1 , ϕ_β and Ψ_2 were computed exactly. By matching the left tail with the central part, described by the β -TW distribution (20), it is possible – as discussed above – to deduce from (48) the higher order asymptotic expansion of \mathcal{F}'_β as [52]

$$\mathcal{F}'_\beta(x) \underset{x \rightarrow -\infty}{\sim} \tau_\beta |x|^{\frac{\beta^2 + 4 - 6\beta}{16\beta}} \exp\left[-\beta \frac{|x|^3}{24} + \sqrt{2} \frac{\beta - 2}{6} |x|^{3/2}\right], \quad (49)$$

which generalizes the result of Ref. [77] valid for $\beta = 1, 2$ and 4 to any real value of $\beta > 0$ (including the constant τ_β which can be computed explicitly for any real value of β [52]).

Right large deviation tail ($w > \sqrt{2}$): The leading order large N saddle point solution in the previous subsection yields a nontrivial left rate function $\Phi_-(w)$ associated with $F_N(w)$ (47) for $w < \sqrt{2}$, corresponding to the *unstable* phase of May's model, but provides only a trivial answer $F_N(w) \sim 1$ for $w > \sqrt{2}$ (i.e., in the *stable* phase of May's model). This is actually very similar to the QCD model in 2-d, where it is known [57, 78] that the saddle point solution gives nontrivial $1/N$ corrections to the free energy only in the strong coupling phase (analogue of the unstable phase), while it gives a trivial result in the weak coupling phase (analogue of the stable phase). The deep reason for this is that in the weak coupling phase the corrections to the free energy are essentially *non-perturbative* that can not be captured via an $1/N$ expansion of the free energy [78]. In gauge theory, these non-perturbative corrections correspond to instanton solutions [78, 79]. In the present case, to capture the nontrivial non-perturbative corrections in the stable phase ($w > \sqrt{2}$) and go beyond the trivial lowest order result $F_N(w) \sim 1$, we need to find a similar “instanton-like” strategy which is outlined below.

Following [48], the right strategy turns out to consider directly the PDF of λ_{\max} , rather than its CDF $F_N(w)$. Taking derivative of (10) with respect to w yields an exact

expression for the PDF of λ_{\max} ,

$$\mathcal{P}(\lambda_{\max} = w, N) \propto e^{-N\beta\frac{w^2}{2}} \int_{-\infty}^w d\lambda_1 \cdots \int_{-\infty}^w d\lambda_{N-1} e^{\beta\sum_{j=1}^{N-1} \ln(|w-\lambda_j|)} P_{\text{joint}}(\lambda_1, \dots, \lambda_{N-1}), \quad (50)$$

where $P_{\text{joint}}(\lambda_1, \dots, \lambda_{N-1})$ is the joint PDF given in (5) for $(N-1)$ eigenvalues. The idea then is to evaluate this $(N-1)$ -fold integral via the saddle point method, for a fixed $w - \sqrt{2} \sim \mathcal{O}(1)$. In this case, one expects that only one (out of a large number N) charge at $w - \sqrt{2} \sim \mathcal{O}(1)$ does not disturb (to leading order) the equilibrium configuration of the rest $(N-1)$ charges whose density then still remains of the standard semi-circular form (45) (see Fig. 4). Following this physical picture, the multiple $(N-1)$ -fold integral in (50) is then well approximated by $\langle e^{\beta\sum_{j=1}^{N-1} \ln(w-\lambda_j)} \rangle$ where the angular brackets denote an average evaluated at the saddle point with semi-circular density. To leading order in large N , one can further replace the average of the exponential by the exponential of the average $e^{\langle \beta\sum_{j=1}^{N-1} \ln(w-\lambda_j) \rangle}$. This gives [48]

$$\mathcal{P}(\lambda_{\max} = w, N) \propto \exp \left[-\beta N \frac{w^2}{2} + \beta N \int \ln |w - \lambda| \tilde{\rho}_{\text{sc}}(\lambda) d\lambda \right], \quad (51)$$

where $\tilde{\rho}_{\text{sc}}(\lambda) = (1/\pi)\sqrt{2 - \lambda^2}$. Thus, one gets to leading order for large N

$$\mathcal{P}(\lambda_{\max} = w, N) \sim \exp[-\beta N \Phi_+(w)], \quad (52)$$

where the right rate function $\Phi_+(w)$ is given by, up to an overall normalization constant

$$\Phi_+(w) = \frac{w^2}{2} - \int_{-\sqrt{2}}^{\sqrt{2}} \ln(|w - \lambda|) \rho_{\text{sc}}(\lambda) d\lambda + A, \quad w > \sqrt{2}, \quad (53)$$

where the constant A is computed such that $\Phi_+(w = \sqrt{2}) = 0$, since our reference configuration is the one where $\lambda_{\max} = \sqrt{2}$. Evaluating the integral in (53), one obtains the result for $\Phi_+(w)$ given in (23).

Thus physically, the quantity $\beta N \Phi_+(w)$ in the right tail of the PDF of λ_{\max} just corresponds to the energy cost ΔE in *pulling* the rightmost charge out of the Wigner sea (see Fig. 5). Since only one charge goes out of the Wigner sea (and it does not lead to a re-organization of the rest of $(N-1)$ charges as in the case $w < \sqrt{2}$), the energy cost ΔE is of order $\mathcal{O}(N)$ and is estimated in (53) by computing the energy of the rightmost charge in the external quadratic potential and its Coulomb interaction energy with the rest of the Wigner sea.

To compute the higher order corrections to the right tail one needs more sophisticated techniques. These were obtained in [53] for $\beta = 2$, using a method based on orthogonal polynomials over the unusual interval $(-\infty, w]$ and adapting a technique originally developed in the context of QCD [78]. It was found [53] that

$$\frac{d}{dw} F_N(w) \sim \frac{e^{-2N\Phi_+(w)}}{2\pi\sqrt{2}(w^2 - 2)}, \quad w > \sqrt{2}, \quad (54)$$

which, by matching with the central part (20), yields the asymptotic behavior of $\mathcal{F}'_2(x)$ beyond the leading order given in (18). One can show that it agrees with the rigorous

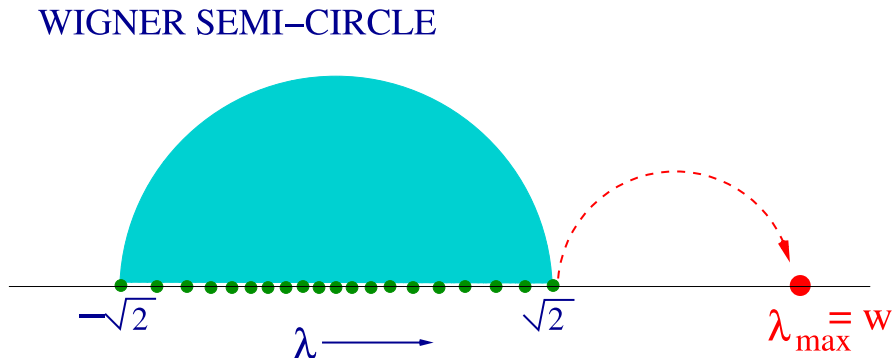


Figure 5. The right rate function is evaluated by computing the energy cost in *pulling* a single charge at $w - \sqrt{2} \sim O(1)$ out of the Wigner sea to its right.

result found in Ref. [80] for the right tail of the β -TW distribution:

$$1 - \mathcal{F}_\beta(x) = x^{-\frac{3\beta}{4} + o(1)} e^{-\frac{2}{3}\beta x^{3/2}}, \quad (55)$$

which was obtained using the stochastic Airy operator representation (17). Very recently, the right large deviation behavior of λ_{\max} has been computed to all orders in N by a generalized loop equation method by Borot and Nadal [55] (see also Ref. [54]). Finally, the unusual orthogonal polynomial method developed in Ref. [53] has recently been extended and generalized to matrix models with higher order critical points [81, 82].

4. Third order phase transitions in other physical models

The third order phase transition, discussed in detail above for $F_N(w)$ in the context of the top eigenvalue of Gaussian random matrices (25), also occurs in various other contexts. We have already mentioned that this transition is very similar to the one found in 2-d lattice QCD, the so called Gross-Witten-Wadia transition [57, 58]. It also appears in the continuum QCD model in two dimensions—the so called Douglas-Kazakov transition [59]. Recently, similar third order transition has been found in the large deviation function associated with the distribution of the maximum height of a set of non-intersecting Brownian excursions in one dimension [34, 61], the distribution of conductance through mesoscopic cavities [83, 84, 85] and the distribution of Renyi entanglement entropy in a bipartite random pure state [86, 87] (see also Refs. [88, 89] for a slightly different description of the same physical system in terms of the Laplace transform of the distribution of purity)—these three cases will be discussed in some detail in this section. In addition, similar third order phase transitions have been noted in models of information propagation through multiple input multiple output (MIMO) channels [90], in the behavior of the complexity in simple spin glass models [46], and more recently in the combinatorial problem of random tilings [91]. We will see later that all these different problems share a common mechanism behind the third order phase

transition— it happens when the gap, between the soft edge of the Coulomb charge density (supported over a single interval) with a square-root singularity at its edge and a hard wall, vanishes as a control parameter (for instance the coupling strength α in May’s model (1) or the gauge field coupling g in 2-d lattice QCD) crosses a critical value.

4.1. Maximal height of N non-intersecting Brownian excursions

We consider N non-intersecting Brownian motions on a line, $x_1(\tau) < x_2(\tau) \cdots < x_N(\tau)$ with an absorbing boundary condition in $x = 0$. In addition, the walkers start in the vicinity of the origin and are conditioned to return to the origin exactly at $\tau = 1$ (see Fig. 6). Such configurations of Brownian motions are called non-intersecting Brownian excursions [92], or sometimes “watermelons with a wall” [93]. An interesting observable is the so called height of the watermelon, which has been studied in the past years by several authors [34, 35, 93, 94, 95, 96, 97, 98, 99] (see also [100] for a related quantity in the context of Dyson’s Brownian motion).

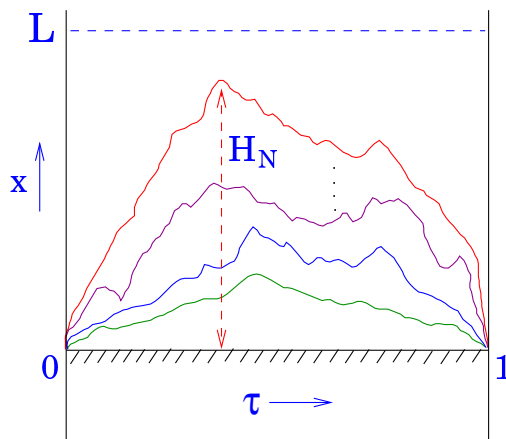


Figure 6. Trajectories of N non-intersecting Brownian motions $x_1(\tau) < x_2(\tau) < \dots < x_N(\tau)$, all start at the origin and return to the origin at $\tau = 1$, staying positive in between. $\tilde{F}_N(L)$ denotes the probability that the maximal height $H_N = \max_{\tau} \{x_N(\tau), 0 \leq \tau \leq 1\}$ stays below the level L over the time interval $0 \leq \tau \leq 1$.

The height H_N of the watermelon is defined as the maximal displacement of the topmost path in this (half-) watermelon configuration, i.e.

$$H_N = \max_{\tau} [x_N(\tau), \tau \in [0, 1]] . \quad (56)$$

The CDF of H_N was computed exactly in Ref. [94] using a Fermionic path integral (see

also [95, 97] for related computations using different methods), yielding the result

$$\begin{aligned} \tilde{F}_N(L) &:= \text{Prob.} [H_N \leq L] \\ &= \frac{A_N}{L^{2N^2+N}} \sum_{n_1=-\infty}^{\infty} \dots \sum_{n_N=-\infty}^{\infty} \Delta^2(n_1^2, \dots, n_N^2) \left(\prod_{j=1}^N n_j^2 \right) e^{-\frac{\pi^2}{2L^2} \sum_{j=1}^N n_j^2}, \end{aligned} \quad (57)$$

where $\Delta_N(y_1, \dots, y_N)$ is the Vandermonde determinant (31) and where A_N is a normalization constant. In Ref. [34] it was shown that this CDF in the Brownian motion model (57) maps onto the exactly solvable partition function (up to a multiplicative pre-factor) of a two-dimensional Yang-Mills gauge theory. More precisely, if one denotes by $\mathcal{Z}(A, G)$ the partition function of the two-dimensional (continuum) Yang-Mills theory on the sphere (denoted as YM_2) with gauge group G and area A , it was shown in Ref. [34] that $\tilde{F}_N(L)$ is related to YM_2 with the gauge group $G = \text{Sp}(2N)$ via the relation

$$\tilde{F}_N(L) \propto \mathcal{Z} \left(A = \frac{2\pi^2}{L^2} N, \text{Sp}(2N) \right). \quad (58)$$

In Ref. [59, 101], it was shown that for large N , $\mathcal{Z}(A, \text{Sp}(2N))$ exhibits a third order phase transition at the critical value $A = \pi^2$ separating a weak coupling regime for $A < \pi^2$ and a strong coupling regime for $A > \pi^2$. This is the so called Douglas-Kazakov phase transition [59], which is the counterpart in continuum space-time, of the Gross-Witten-Wadia transition [57, 58] discussed above which is also of third order. Using the correspondence $L^2 = 2\pi^2 N/A$, we then find that $\tilde{F}_N(L)$, considered as a function of L with N large but fixed, also exhibits a third order phase transition at the critical value $L_c(N) = \sqrt{2N}$. Furthermore, the weak coupling regime ($A < \pi^2$) corresponds to $L > \sqrt{2N}$ and thus describes the right tail of $\tilde{F}_N(L)$, while the strong coupling regime corresponds to $L < \sqrt{2N}$ and describes instead the left tail of $\tilde{F}_N(L)$ (see Fig. 7). This is thus qualitatively very similar to the stability diagram of model (1) depicted in Fig. 1. The critical regime around $A = \pi^2$ is the so called ‘‘double scaling’’ limit in the matrix model and has width of order $N^{-2/3}$. It corresponds to the region of width $\mathcal{O}(N^{-1/6})$ around $L = \sqrt{2N}$ where $\tilde{F}_N(L)$, correctly shifted and scaled, is described by the Tracy-Widom distribution $\mathcal{F}_1(x)$ [34, 35] given in (16).

In Refs. [34, 61] the three regimes for $\tilde{F}_N(L)$ (the left tail, the central part and the right tail) were studied in detail, yielding the results

$$\mathcal{P}(H_N = L) \approx \begin{cases} \exp \left[-N^2 \phi_-^A \left(L/\sqrt{2N} \right) \right], & L < \sqrt{2N} \ \& \ |L - \sqrt{2N}| \sim \mathcal{O}(\sqrt{N}) \\ 2^{11/6} N^{1/6} \mathcal{F}'_1 \left[2^{11/6} N^{1/6} (L - \sqrt{2N}) \right], & |L - \sqrt{2N}| \sim \mathcal{O}(N^{-1/6}) \\ \exp \left[-N \phi_+^A \left(L/\sqrt{2N} \right) \right], & L > \sqrt{2N} \ \& \ |L - \sqrt{2N}| \sim \mathcal{O}(\sqrt{N}), \end{cases} \quad (59)$$

where \mathcal{F}_1 is the TW distribution for GOE (16). The rate functions $\phi_{\pm}^A(x)$ can be computed exactly [61]: of particular interest are their asymptotic behaviors when

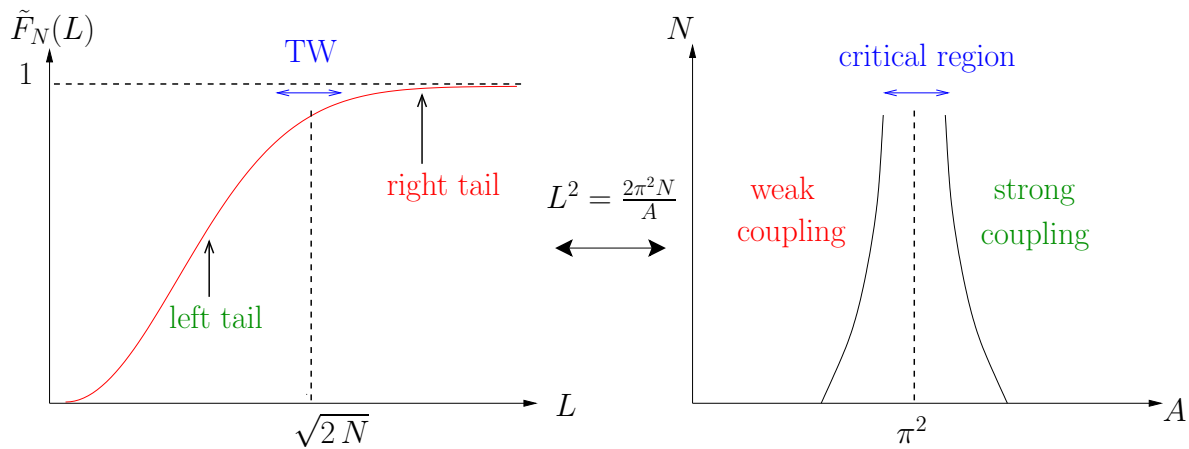


Figure 7. Left: Schematic sketch of the CDF of H_N , $\tilde{F}_N(L)$ as defined in (57) for N vicious walkers on the line segment $[0, L]$ with an absorbing boundary condition in $x = 0$. **Right:** Sketch of the phase diagram in the plane (A, N) of two-dimensional Yang-Mills theory on a sphere with the gauge group $\text{Sp}(2N)$ as obtained in Ref. [59, 101]. The weak (strong) coupling phase in the right panel corresponds to the right (left) tail of $\tilde{F}_N(L)$ in the left panel. The critical region around $A = \pi^2$ in the right panel corresponds to the Tracy-Widom (TW) regime in the left panel around the critical point $L_c(N) = \sqrt{2N}$.

$L \rightarrow \sqrt{2N}$ from below (left tail) and from above (right tail), which are given by

$$\begin{aligned} \phi_-^A(x) &\sim \frac{16}{3}(1-x)^3, \quad x \rightarrow 1^-, \\ \phi_+^A(x) &\sim \frac{2^{9/2}}{3}(x-1)^{3/2}, \quad x \rightarrow 1^+. \end{aligned} \quad (60)$$

The different behavior of the CDF $\tilde{F}_N(L)$ of the maximal height in the Brownian motion problem (59) is thus formally very similar to the behavior of the CDF of λ_{\max} for Gaussian random matrices (20). In addition, the behavior of $\tilde{F}_N(L)$ for $L < \sqrt{2N}$ and $L > \sqrt{2N}$ leads also here, in the limit $N \rightarrow \infty$, to a phase transition at the critical point $L = \sqrt{2N}$ in the following sense. Indeed if one scales L by $\sqrt{2N}$, keeping the ratio $x = L/\sqrt{2N}$ fixed, and take the limit $N \rightarrow \infty$ one obtains

$$\lim_{N \rightarrow \infty} -\frac{1}{N^2} \ln \tilde{F}_N \left(x = \frac{L}{\sqrt{2N}} \right) = \begin{cases} \phi_-^A(x), & x < 1 \\ 0 & x > 1. \end{cases} \quad (61)$$

If one interprets $\tilde{F}_N(L)$ in (57) as the partition function of a discrete Coulomb gas, its logarithm can be interpreted as its free energy. Since $\phi_-^A(x) \sim (1-x)^3$ when x approaches 1 from below, then the third derivative of the free energy at the critical point $x = 1$ is discontinuous, which can also be interpreted as a third order phase transition, similar (albeit with different details) to the one found for the largest eigenvalue of Gaussian random matrices (22, 25). Notice also that, thanks to the asymptotic behaviors

of the rate functions (60), one can show that the matching between the different regimes is similar to the one found for λ_{\max} and discussed above in section 2.3.

4.2. Conductance and shot noise in mesoscopic cavities

The second example concerns the large deviation formulas for linear statistics of the N transmission eigenvalues T_i of a chaotic cavity, in the framework of RMT. We consider here the statistics of quantum transport of electrons through a mesoscopic cavity, such as a quantum dot. This chaotic cavity is connected to two identical leads, each supporting N channels. An electron, injected in the cavity through one lead, gets scattered in the cavity and leaves it by either of the two leads. In the Landauer-Büttiker approach [102, 103, 104], the transport of electrons through such an open quantum system is encoded by the $2N \times 2N$ unitary scattering matrix

$$S = \begin{pmatrix} r & t' \\ t & r' \end{pmatrix}, \quad (62)$$

where the transmission (t, t') and reflection (r, r') blocks are $N \times N$ matrices encoding the transmission and reflection coefficients among different channels. Several physically relevant transport observables, such as the conductance G , or the shot noise power P can be expressed in terms of the transmission eigenvalues T_i 's of the $N \times N$ matrix $T = tt^\dagger$. One has, for instance, for G [103] and P [104]

$$G = \text{Tr}(tt^\dagger) = \sum_{i=1}^N T_i, \quad P = \text{Tr}(tt^\dagger(1 - tt^\dagger)) = \sum_{i=1}^N T_i(1 - T_i), \quad (63)$$

where $0 \leq T_i \leq 1$ denotes the probability that an electron gets transmitted through the channel i . Over the past two decades, RMT has been successfully used [102] to model the transport through such a cavity. Within this approach, one assigns a uniform probability density to all scattering matrices S belonging to the unitary group: the matrix S is thus drawn from one of Dyson's circular ensembles [3, 11]. It is then possible, though non trivial, to derive the joint PDF of the transmission eigenvalues T_i which reads [102]:

$$\tilde{P}_{\text{joint}}(T_1, \dots, T_N) = \tilde{B}_N(\beta) \Delta_N^\beta(T_1, \dots, T_N) \prod_{i=1}^N T_i^{\frac{\beta}{2}-1}, \quad 0 \leq T_i \leq 1 \quad \forall i, \quad (64)$$

where $\tilde{B}_N(\beta)$ is a normalization constant and the Dyson index characterizes the different symmetry classes ($\beta = 1, 2$ according to the presence or absence of time reversal symmetry and $\beta = 4$ in case of spin-flip symmetry).

While formal expressions for the distributions of the conductance $\mathcal{P}_N(G)$ and of the shot noise power $\mathcal{P}_N(P)$, for arbitrary finite N and β , were obtained in Refs. [105, 106] and an exact recursion relation for the cumulants of the conductance distribution was obtained in Ref. [107], it is not easy to obtain the large N asymptotics of these results: indeed, the asymptotic tails of the conductance distribution derived in Ref. [107] by extrapolation of these finite N cumulants turned out to be incorrect (as was demonstrated in [83, 84]). It turns out that an easier method to derive directly the

large N results is via using the Coulomb gas method [83, 84], where T_i 's (distributed via the joint PDF (64)) can be interpreted as the position of the i -th charge confined in a finite box $T_i \in [0, 1]$, repelling each other via the Vandermonde term and each subjected to an external potential. The probability density of any linear statistic of T_i 's can then be analyzed by performing a saddle point analysis of the underlying Coulomb gas in the large N limit [83, 84]. Skipping details, it was found that for both distributions $\mathcal{P}_N(G)$ and $\mathcal{P}_N(P)$, there is a central Gaussian region flanked on both sides by non-Gaussian tails. For the conductance, $\mathcal{P}_N(G)$ behaves as

$$\mathcal{P}_N(G) \approx \exp \left[-\frac{\beta}{2} N^2 \Psi_G \left(\frac{G}{N} \right) \right], \quad \Psi_G(x) = \begin{cases} \frac{1}{2} - \ln(4x), & 0 \leq x \leq \frac{1}{4} \\ 8 \left(x - \frac{1}{2}\right)^2, & \frac{1}{4} \leq x \leq \frac{3}{4} \\ \frac{1}{2} - \ln[4(1-x)], & \frac{3}{4} \leq x \leq 1 \end{cases}, \quad (65)$$

and a similar (with slightly different details) behavior was found for $\mathcal{P}_N(P)$, with an associated rate function $\Psi_P(x)$. It turns out that at the two singular points $G/N = 1/4$ and $G/N = 3/4$, the underlying saddle point charge density $\rho^*(x)$ changes form. Exactly at the two critical points, one edge of the Coulomb gas with density vanishing at the edge as a square-root hits the hard physical boundary of the bounding box at 0 and 1 respectively [83, 84]. Consequently, the system undergoes a third order phase transition at $G/N = 1/4$ and also at $G/N = 3/4$. Indeed, one can check from (65) that the third derivative of the rate function $\Psi_G(x)$ is discontinuous at these critical points. Such a third order phase transition also occurs for the distribution of the shot noise power [83] and is expected to occur for any generic linear statistics of the eigenvalues T_i 's [84]. These non-analyticities of the rate functions thus appear as a direct consequence of phase transitions in the associated Coulomb gas problems. The existence of these three different regimes (65) were confirmed by numerical simulations [83, 84]. Finally, we note that similar large deviations regimes [albeit with an additional fourth regime compared to (65)] and associated third order phase transitions were found for the Andreev conductance of a metal-superconductor interface in Ref. [85].

4.3. Bipartite entanglement of a random pure state

Another example of a third order phase transition is provided by the distribution of the bipartite entanglement of a random pure state. We consider a bipartite quantum system which is described by the tensorial product of two smaller Hilbert spaces $\mathcal{H}_A \otimes \mathcal{H}_B$. We denote by N and M the dimensions of \mathcal{H}_A and \mathcal{H}_B and introduce $c = N/M$, with $0 < c \leq 1$. We are mainly interested in the case where both M and N are large. The limit $c = 1$ corresponds to $M = N$ while $c \rightarrow 0$ corresponds to the case where B is the environment (e.g. a thermostat) and A the system of interest. Here we focus on the case $c = 1$. We suppose that the full system $A \otimes B$ is described by a random pure state $|\psi\rangle$ (such that $\langle\psi|\psi\rangle = 1$) and we denote by $\rho = |\psi\rangle\langle\psi|$ the associated density matrix, satisfying $\text{Tr}[\rho] = 1$. We are interested in the entanglement entropy and hence we consider the reduced density matrices $\rho_A = \text{Tr}_B[\rho]$ and $\rho_B = \text{Tr}_A[\rho]$. These

two matrices ρ_A and ρ_B share the same non-negative eigenvalues $\lambda_1, \dots, \lambda_N$ with the normalization constraint $\sum_{i=1}^N \lambda_i = 1$. If we denote by $|\lambda_i^A\rangle$ and $|\lambda_i^B\rangle$ the corresponding eigenvectors of ρ_A and ρ_B , an arbitrary pure state $|\psi\rangle$ can be written in the so called Schmidt basis:

$$|\psi\rangle = \sum_{i=1}^N \sqrt{\lambda_i} |\lambda_i^A\rangle \otimes |\lambda_i^B\rangle. \quad (66)$$

As an example, let us consider two limiting cases: (i) if $\lambda_j = 1$ and the remaining $N - 1$ eigenvalues are identically zero, then $|\psi\rangle = \lambda_j |\lambda_j^A\rangle \otimes |\lambda_j^B\rangle$. Hence the state factorizes and the system is completely unentangled. (ii) If instead all the eigenvalues are equal, $\lambda_i = 1/N$ for all i , all the states are equally represented in (66) and the state is maximally entangled. A standard measure of entanglement is provided by the von Neumann entropy, $S_{\text{VN}} = -\sum_{i=1}^N \lambda_i \ln \lambda_i$ [it takes its minimum value 0 in case (i) and its maximal value $\ln N$ in case (ii)]. Another useful measure of entanglement is provided by the Renyi's entropies

$$S_q = \frac{1}{q-1} \ln \Sigma_q, \quad \Sigma_q = \sum_{i=1}^N \lambda_i^q, \quad (67)$$

and we restrict here our analysis to the case $q \geq 1$. S_q is also minimal in case (i) where $S_q = 0$ and maximal for case (ii) where $S_q = \ln N$. Note that $S_q \rightarrow S_{\text{VN}}$ when $q \rightarrow 1$ while $S_q \rightarrow -\ln \lambda_{\max}$ when $q \rightarrow \infty$ (where $\lambda_{\max} = \max_{1 \leq i \leq N} \lambda_i$). If the random pure state $|\psi\rangle$ is uniformly distributed (i.e. according to the uniform Haar measure) the eigenvalues λ_i 's are also random variables with the joint PDF given by [108]

$$\mathcal{P}_{\text{joint}}^W(\lambda_1, \dots, \lambda_N) = \mathcal{B}_N^W(\beta) \prod_{i=1}^N \lambda_i^{\beta-1} \Delta_N^\beta(\lambda_1, \dots, \lambda_N) \delta\left(\sum_{i=1}^N \lambda_i - 1\right), \quad (68)$$

where $\Delta_N(\lambda_1, \dots, \lambda_N)$ is the Vandermonde determinant (31) and $\mathcal{B}_N^W(\beta)$ a normalization constant. Here $\beta = 2$ and the δ -function enforces the constraint that $\text{Tr}[\rho_A] = 1$. Note that, apart from this constraint, this joint PDF (68) is identical to the eigenvalue distribution of random Gaussian Wishart matrices (30).

In Refs. [86, 87], the PDF of Σ_q [which yields the PDF of S_q itself from (67)] was computed using Coulomb gas techniques similar to the ones explained above in section 3 for all q . For the special case $q = 2$, the Laplace transform of the distribution of purity $\sum_{i=1}^N \lambda_i^2$ was studied by similar methods in Refs. [88, 89]. The main results obtained in Refs. [86, 87] can be summarized as follows. First, due to the global constraint, $\sum_{i=1}^N \lambda_i = 1$, one deduces that the typical scale of λ_i 's is $\mathcal{O}(1/N)$ and hence $\Sigma_q \sim \mathcal{O}(N^{1-q})$. Note also that for $q \geq 1$, one has necessarily $N^{1-q} \leq \Sigma_q \leq 1$. It was further shown in Refs. [86, 87] that the PDF $\mathcal{P}(\Sigma_q = N^{1-q}s)$ displays three different regimes: the distribution has indeed a Gaussian peak [centered on the mean value $\bar{s}(q)$] flanked on both sides by two non-Gaussian tails. There are thus three different regimes

separated by two critical values $s_1(q)$ and $s_2(q)$ such that

$$\mathcal{P}(\Sigma_q = N^{1-q}s) \approx \begin{cases} \exp[-\beta N^2 \Phi_I(s)], & 1 \leq s \leq s_1(q) \\ \exp[-\beta N^2 \Phi_{II}(s)], & s_1(q) \leq s \leq s_2(q) \\ \exp\left[-\beta N^{1+\frac{1}{q}} \Phi_{III}(s)\right], & s > s_2(q). \end{cases} \quad (69)$$

Interestingly, at the first critical point $s_1(q)$, the PDF exhibits also a third-order phase transition (i.e. the third derivative of the large deviation function is discontinuous), as found above. On the other hand, at the second critical point $s_2(q)$, a Bose-Einstein type condensation occurs and the distribution changes shape abruptly: in this case the first derivative is discontinuous in the limit $N \rightarrow \infty$. Here also, these changes of behavior (69) are a direct consequence of two phase transitions in the associated Coulomb gas problem, and more precisely in the shape of the optimal charge density [86, 87].

5. Basic mechanism of the third order transition and its generalizations

All the problems discussed so far in this article share one common feature: there is a third order phase transition as a control parameter α crosses a critical value α_c . In the case of May's model of dynamical systems, α denotes the strength of the pairwise interaction between species, whereas in the 2-d lattice QCD, $\alpha = g$ is the coupling strength of the gauge fields. The basic mechanism behind this third order phase transition can be summarized as follows. In all these problems, there is an underlying one dimensional Coulomb gas, with charge density supported over a *single* interval and in presence of a hard wall located at w . The equilibrium charge density of the Coulomb gas $\rho_\alpha(x)$ depends on α . In the *weak coupling* phase ($\alpha < \alpha_c$), $\rho_\alpha(x)$ has typically a soft edge at $x = b < w$ where the density vanishes as a square root, $\rho_\alpha(x) \sim (b - x)^{1/2}$. Thus, in this case, there is a nonzero gap between the soft edge of the Coulomb gas and the hard wall at w , and the charges do not feel the presence of the wall. As α increases and approaches the critical value α_c , the soft edge approaches the hard wall leading to a vanishing gap. For $\alpha > \alpha_c$, the edge of the charge density gets *pushed* by the wall and the systems adjusts itself to a new deformed equilibrium charge density with a nonzero density at the wall location—this is the so called *strong coupling* phase ($\alpha > \alpha_c$) (see Fig. 8).

In all these cases where the charge density vanishes as a square-root at the soft edge of the single support in the weak coupling phase, one obtains a third order phase transition from the weak to strong coupling phase when the tuning parameter crosses the critical value $\alpha = \alpha_c$ from below. For finite but large N , if one zooms in the critical region, one finds a smooth crossover from the weak coupling to the strong coupling phase and the crossover function has the Tracy-Widom scaling form (expressed in terms of a solution of a Painlevé-II differential equation). In fact, in the context of 2-d QCD,

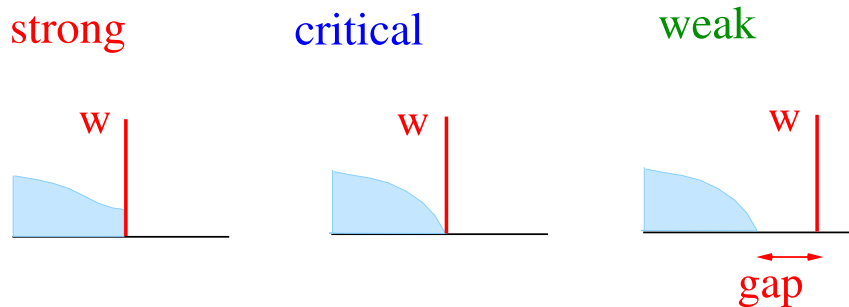


Figure 8. A third order phase transition between a weak coupling and a strong coupling phase occurs when the gap, between the soft edge of a Coulomb droplet with density vanishing as a square-root at the edge and a hard wall at w , vanishes as one tunes a control parameter through its critical value.

this was already noticed by Periwal and Shevitz [109] before the work of Tracy and Widom [17], but there was no probabilistic interpretation of this crossover function. From the work of Tracy and Widom [17], it follows that this crossover function can be interpreted as the centered and scaled limiting distribution of the largest eigenvalue of a Gaussian random matrix.

What happens if the equilibrium charge density vanishes at the soft edge (in the weak coupling phase) not as a square-root, but say as $\tilde{\rho}(x) \sim (b-x)^\gamma$ with an exponent $\gamma > 0$? How does the order of the transition depend on γ ? Indeed, this question arises in the context of higher order critical matrix models [110]. Consider for instance a random $(N \times N)$ matrix X whose entries are drawn from the joint distribution $\text{Prob.}[X] \propto \exp[-N \text{Tr}(V(X))]$ where $V(X)$ is a polynomial potential. By choosing the potential $V(X)$ appropriately, one can engineer equilibrium charge densities that are different from the Wigner semi-circular form [110]. For instance, if one chooses $V(X) = X^4/20 - 4X^3/15 + X^2/5 + 8X/5$ and with $\beta = 2$, the saddle point charge density can be computed exactly [111, 112]

$$\tilde{\rho}(x) = \frac{1}{10\pi}(x+2)^{1/2}(2-x)^{5/2}, \quad x \in [-2, 2], \quad (70)$$

which thus vanishes with an exponent $\gamma = 5/2$ at the upper soft edge $b = 2$. For such matrix models with a higher order critical point, the distribution of the typical fluctuations of the largest eigenvalue around its mean b are described by higher-order analogues of the Tracy-Widom distribution [111, 112]. One also expects that there would be the analogues of the large deviation functions of λ_{\max} , just as in the simple quadratic case $V(X) = X^2/2$ discussed in Section 2 and these large deviation rate functions (both left and right) have recently been computed using generalized orthogonal polynomial techniques [81, 82]. Clearly there would be a phase transition in the CDF of λ_{\max} at the critical value $\lambda_{\max} = b$ for these critical matrix models as well. What is the order of

this phase transition? This order can be easily estimated by the following simple scaling argument.

Let, in general, $\tilde{\rho}(x) \sim (b-x)^\gamma$ at the upper soft edge $x = b$. One can easily estimate the scale of typical fluctuation $\delta\lambda_{\max}$ of λ_{\max} around its mean b . Using the standard EVS criterion [see Eq. (12)], i.e., setting $\int_{b-\delta\lambda_{\max}}^b \tilde{\rho}(x)dx \sim 1/N$, one gets

$$\delta\lambda_{\max} = b - \lambda_{\max} \sim \mathcal{O}(N^{-1/(1+\gamma)}) . \quad (71)$$

For $\gamma = 1/2$, one recovers $\delta\lambda_{\max} \sim \mathcal{O}(N^{-2/3})$. Hence, one would expect that on this scale, the CDF of λ_{\max} will have the scaling form

$$\text{Prob.}[\lambda_{\max} \leq w] \sim \mathcal{F}(N^{1/(1+\gamma)}(w-b)) , \quad (72)$$

where the scaling function $\mathcal{F}(x)$ is the γ -analogue of the Tracy-Widom function. Now, in general, we would expect that far in the left tail, this function should decay asymptotically as,

$$\mathcal{F}(x) \sim \exp[-a_0 |x|^\delta] , \text{ for } x \rightarrow -\infty , \quad (73)$$

where a_0 is a constant. Clearly, for $\gamma = 1/2$ case (i.e., when $\mathcal{F}(x)$ is the standard Tracy-Widom), one has $\delta = 3$ [see Eq. (18)].

On the other hand, it follows from the general Coulomb gas argument in Section 3 that atypical fluctuations of λ_{\max} of $\sim \mathcal{O}(1)$ to the left of b , i.e., when $w < b$, are described by a large deviation form

$$\text{Prob.}[\lambda_{\max} \leq w] \sim \exp[-\beta N^2 \Phi_-(w)] , \quad w < b , \quad (74)$$

where $\Phi_-(w)$ is a rate function that should vanish as $w \rightarrow b$ from the left. Interpreting $\Phi_-(w)$ as the free energy as in the Gaussian case, we then expect $\Phi_-(w) \sim a_1 (b-w)^\sigma$ as $w \rightarrow b$ where a_1 is a constant and the exponent σ then decides the order of the transition. To estimate σ , we match this left large deviation results (when $w \rightarrow b$) with the extreme left tail of the central peak region as described in (73). Substituting $\Phi_-(w) \sim a_1 (b-w)^\sigma$ in (74) gives, for $w \rightarrow b$,

$$\begin{aligned} \text{Prob.}[\lambda_{\max} \leq w] &\sim \exp[-\beta N^2 a_1 (b-w)^\sigma] , \\ &\sim \exp[-\beta a_1 [N^{2/\sigma} (b-w)]^\sigma] . \end{aligned} \quad (75)$$

In contrast, for $(b-w) \gg N^{-1/(1+\gamma)}$, we get, by using the left tail asymptotics (73) of the central peak behavior in (72),

$$\text{Prob.}[\lambda_{\max} \leq w] \sim \exp[-a_0 \{N^{1/(1+\gamma)} (b-w)\}^\delta] . \quad (76)$$

Assuming that the two behaviors merge smoothly, we find by comparing (75) and (76)

$$\delta = \sigma \text{ and } \frac{\delta}{1+\gamma} = 2 , \quad (77)$$

which then relates the order of the transition σ to the exponent γ characterizing the vanishing of the charge density at the soft edge, via the simple scaling relation

$$\sigma = 2(1+\gamma) . \quad (78)$$

For example, for $\gamma = 1/2$, one recovers the third order transition $\sigma = 3$. As an example, the case (70) with $\gamma = 5/2$, will then have a seventh order ($\sigma = 7$) phase transition.

6. Conclusion

To summarize, we have provided a rather complete understanding of the behavior of the probability distribution of the top eigenvalue λ_{\max} of an $N \times N$ Gaussian random matrix for large N . While the typical small fluctuations of λ_{\max} of order $\sim \mathcal{O}(N^{-2/3})$ around its mean $\lambda_{\max} = \sqrt{2}$ are described by Tracy-Widom distributions, atypically large fluctuations of $\sim \mathcal{O}(1)$ are described by two different large deviation functions respectively on the left and on the right of the mean. These two tails correspond to very different physics in terms of the underlying Coulomb gas describing the eigenvalues: the left large deviation corresponds to a *pushed* Coulomb gas, while the right large deviation corresponds to a *pulled* Coulomb gas. We have shown that the left large deviation function can be interpreted as a thermodynamic free energy and that it undergoes a third order phase transition at $\lambda_{\max} = \sqrt{2}$, i.e, its third derivative is discontinuous at $\lambda_{\max} = \sqrt{2}$. This result provides a thermodynamic meaning to the stable-unstable phase transition in May's model of dynamical systems. Furthermore, it shows that this phase transition occurs in a broad class of systems ranging from dynamical systems all the way to two dimensional gauge theory. The *pushed* phase (i.e., the *unstable* phase in May's model) corresponds to the *strong coupling* phase of the gauge theory, while the *pulled* phase (i.e., the *stable* phase in May's model) corresponds to the non-perturbative *weak coupling* phase of the gauge theory. In addition, several other physical systems with a similar third order phase transition have been discussed. The basic mechanism behind this transition is also identified: it happens when the gap between the soft edge characterizing the equilibrium charge density of an underlying Coulomb gas with a single support and a hard wall vanishes. The generalizations to higher order phase transitions have also been discussed.

The main interesting point to note is that the large deviation function associated with the probability distribution of an observable \hat{O} of an $(N \times N)$ random matrix, such as the largest eigenvalue $\hat{O} = \lambda_{\max}$ or other linear statistics of the form $\hat{O} = \sum_{i=1}^N f(\lambda_i)$ (where $f(x)$ is an arbitrary function), may exhibit singularities in the large N limit and these singularities typically signal a phase transition in the underlying Coulomb gas. Hence, these large deviation functions are indeed the analogues of the thermodynamic free energy in a standard statistical mechanical system. Here we have discussed several cases where these singularities are of the power-law variety, i.e., vanishes as some power near the critical point. However, other cases with essential singularities [36] and logarithmic singularities [113, 114, 115] have also been identified. In addition, in several examples a first order phase transition (akin to Bose-Einstein condensation) has been shown to take place when a single eigenvalue splits off the sea of eigenvalues [87, 116]. Finally, we note that recently a third order phase transition has been found in two dimensions [117]—in the large deviation function associated with the index distribution in real and complex Ginibre random matrices. The mechanism for this third order transition in two dimensions (where the charge density in the complex plane has two supports) seems to be different from the one dimensional cases with a single support

discussed in this article.

In conclusion, the large deviation functions associated with the probability distribution of an observable in RMT carry crucial informations concerning phase transitions in the system in the form of singularities and hence are useful and important objects to study.

Acknowledgments

This review is dedicated to the memory of Oriol Bohigas from whom we learnt many aspects of random matrix theory. We would also like to thank R. Allez, G. Akemann, J. Baik, G. Ben Arous, O. Bohigas, G. Borot, J.-P. Bouchaud, A. Comtet, K. Damle, D. S. Dean, D. Dhar, B. Eynard, P. J. Forrester, A. Lakshminarayan, C. Nadal, S. Nechaev, J. Rambeau, A. Scardicchio, C. Texier, S. Tomsovic, V. Tripathi, M. Vergassola, D. Villamaina, P. Vivo, G. Wainrib, O. Zeitouni for useful discussions and collaborations. We acknowledge support by ANR grant 2011-BS04-013-01 WALKMAT and in part by the Indo-French Centre for the Promotion of Advanced Research under Project 4604-3.

- [1] J. Wishart, *Biometrika* **20**, 32 (1928).
- [2] E. Wigner, *Proc. Cambridge Philos. Soc.* **47**, 790 (1951).
- [3] M. L. Mehta, *Random Matrices*, 2nd Edition, Academic Press (1991).
- [4] G. Akemann, J. Baik, P. Di Francesco, eds. *The Oxford handbook of random matrix theory*, Oxford Univ. Press, Oxford, (2011).
- [5] J.-P. Bouchaud, M. Mézard, *J. Phys. A* **30**, 7997 (1997).
- [6] D. S. Dean, S. N. Majumdar, *Phys. Rev. E* **64**, 046121 (2001).
- [7] P. Le Doussal, C. Monthus, *Physica A* **317**, 140 (2003).
- [8] E. J. Gumbel, *Statistics of Extremes*, Columbia University Press, (1958).
- [9] R. M. May, *Nature* **238**, 413 (1972).
- [10] M. R. Gardner, W. R. Ashby, *Nature* **228**, 784 (1970).
- [11] P. J. Forrester, *Log-gases and random matrices*, Princeton University Press, Princeton, NJ, (2010).
- [12] F. J. Dyson, *J. Math. Phys.* **3**, 140 (1962).
- [13] I. Dumitriu, A. Edelman, *J. Math. Phys.* **43**, 5830 (2002).
- [14] D. S. Dean, S. N. Majumdar, *Phys. Rev. Lett.* **97**, 160201 (2006).
- [15] M. Bowick, E. Brézin, *Phys. Lett. B* **268**, 21 (1991).
- [16] P. J. Forrester, *Nucl. Phys. B* **402**(3), 709 (1993).
- [17] C. A. Tracy, H. Widom, *Commun. Math. Phys.* **159**, 151 (1994).
- [18] C. A. Tracy, H. Widom, *Commun. Math. Phys.* **177**, 727 (1996).
- [19] A. Edelman, B. Sutton, *J. Stat. Phys.* **127**(6), 1121 (2007).
- [20] J. Ramirez, B. Rider, B. Virág, *J. Amer. Math. Soc.* **24**, 919 (2011).
- [21] I. M. Johnstone, *Ann. Stat.* **29**, 295 (2001).
- [22] A. Soshnikov, *J. Stat. Phys.* **108**, 1033 (2002).
- [23] K. Johansson, *Commun. Math. Phys.* **209**, 437 (2000).
- [24] S. N. Majumdar, *Les Houches lecture notes on Complex Systems* (2006), ed. by J.-P. Bouchaud, M. Mézard and J. Dalibard [arXiv: cond-mat/0701193].
- [25] J. Baik, P. Deift, K. Johansson, *J. Am. Math. Soc.* **12**, 1119 (1999).
- [26] J. Baik, E. M. Rains, *J. Stat. Phys.* **100**, 523 (2000).
- [27] M. Prähofer, H. Spohn, *Phys. Rev. Lett.* **84**, 4882 (2000); J. Gravner, C. A. Tracy, H. Widom, *J. Stat. Phys.* **102**, 1085 (2001); S. N. Majumdar, S. Nechaev, *Phys. Rev. E* **69**, 011103 (2004); T. Imamura, T. Sasamoto, *Nucl. Phys. B* **699**, 503 (2004).
- [28] T. Sasamoto, H. Spohn, *Phys. Rev. Lett.* **104**, 230602 (2010).
- [29] P. Calabrese, P. Le Doussal, A. Rosso, *Europhys. Lett.* **90**, 20002 (2010).
- [30] V. Dotsenko, *Europhys. Lett.* **90**, 20003 (2010).
- [31] G. Amir, I. Corwin, J. Quastel, *Comm. Pure and Appl. Math.* **64**, 466 (2011).
- [32] S. N. Majumdar, S. K. Nechaev, *Phys. Rev. E* **72**, 020901(R) (2005).
- [33] M. G. Vavilov, P. W. Brouwer, V. Ambegaokar, C. W. J. Beenakker, *Phys. Rev. Lett.* **86**, 874 (2001); A. Lamacraft, B. D. Simons, *Phys. Rev. B* **64**, 014514 (2001); P. M. Ostrovsky, M. A. Skvortsov, M. V. Feigel'man, *Phys. Rev. Lett.* **87**, 027002 (2001); J. S. Meyer, B. D. Simons, *Phys. Rev. B* **64**, 134516 (2001); A. Silva, L. B. Ioffe, *Phys. Rev. B* **71**, 104502 (2005).
- [34] P. J. Forrester, S. N. Majumdar, G. Schehr, *Nucl. Phys. B* **844**, 500 (2011).
- [35] K. Liechty, *J. Stat. Phys.* **147**, 582 (2012).
- [36] C. Nadal, S. N. Majumdar, *Phys. Rev. E*, **79**, 061117 (2009).
- [37] G. Biroli, J.-P. Bouchaud, M. Potters, *Eur. Phys. Lett.* **78**, 10001 (2007).
- [38] K. A. Takeuchi, M. Sano, *Phys. Rev. Lett.* **104**, 230601 (2010); K. A. Takeuchi, M. Sano, T. Sasamoto, H. Spohn, *Sci. Rep. (Nature)* **1**, 34 (2011); K. A. Takeuchi, M. Sano, *J. Stat. Phys.* **147**, 853 (2012).
- [39] M. Fridman, R. Pugatch, M. Nixon, A. A. Friesem, N. Davidson, *Phys. Rev. E* **85**, R020101 (2012).
- [40] A. Aazami, R. Easther, *J. Cosmol. Astropart. Phys.* **0603**, 18 (2006).
- [41] D. Marsh, L. McAllister, T. Wrase, *JHEP* 1203:102 (2012).
- [42] D. Marsh, L. McAllister, E. Pajer, T. Wrase, arXiv: 1307.3559.

- [43] A. J. Bray, D. S. Dean, Phys. Rev. Lett. **98**, 150201 (2007).
- [44] Y. V. Fyodorov, I. Williams, J. Stat. Phys., **129**, 1081 (2007).
- [45] D. S. Dean, S. N. Majumdar, Phys. Rev. E **77**, 041108 (2008).
- [46] Y. V. Fyodorov, C. Nadal, Phys. Rev. Lett. **109**, 167203 (2012).
- [47] Y. V. Fyodorov, Lecture notes for the Summer School: *Randomness in Physics and Mathematics*. ZIF, Bielefeld, (2013), arXiv: 1307.2309 and references therein.
- [48] S. N. Majumdar, M. Vergassola, Phys. Rev. Lett. **102**, 060601 (2009).
- [49] G. Ben Arous, A. Dembo, A. Guionnet, Probab. Theory Relat. Fields **120**, 1 (2001).
- [50] P. J. Forrester, J. Phys. A: Math. Theor. **45**, 075206 (2012).
- [51] Y. V. Fyodorov, Phys. Rev. Lett. **92**, 240601 (2004); Erratum *ibid.* **92**, 240601 (2004).
- [52] G. Borot, B. Eynard, S. N. Majumdar, C. Nadal, J. Stat. Mech. **P11024** (2011).
- [53] C. Nadal, S. N. Majumdar, J. Stat. Mech. **P04001** (2011).
- [54] P. J. Forrester, J. Phys. A **45**, 075206 (2012).
- [55] G. Borot, C. Nadal, J. Phys. A: Math. Theor. **45**, 075209 (2012). Random Matrices: Theory Appl. **01**, 1250006 (2012).
- [56] Y. V. Fyodorov, P. Le Doussal, preprint arXiv:1304.0024, to appear in J. Stat. Phys.
- [57] D. J. Gross, E. Witten, Phys. Rev. D **21**, 446 (1980).
- [58] S. R. Wadia, Phys. Lett. **93B**, 403 (1980).
- [59] M. R. Douglas, V. A. Kazakov, Phys. Lett. B **319**, 219 (1993).
- [60] P. Vivo, S. N. Majumdar, O. Bohigas, J. Phys. A: Math. Theor. **40**, 4317 (2007).
- [61] G. Schehr, S. N. Majumdar, A. Comtet, P. J. Forrester, J. Stat. Phys. **150**(3), 491 (2013).
- [62] A. T. James, Ann. Math. Stat. **35**, 475 (1964).
- [63] V. A. Marčenko, L. A. Pastur, Math. USSR-Sb. **1**, 457 (1967).
- [64] E. Katzav, I. Pérez Castillo, Phys. Rev. E **82**, 040104(R) (2010).
- [65] H. M. Ramli, E. Katzav and I. Pérez Castillo, J. Phys. A: Math. Theor. **45**, 465005 (2012).
- [66] A. Edelman, J. Matrix Anal. and Appl. **9**, 543 (1988); Linear Algebra Appl. **159**, 55 (1991).
- [67] P. J. Forrester, J. Math. Phys. **35**, 2539 (1994).
- [68] S. N. Majumdar, in chapter 37 of the book *The Oxford handbook of random matrix theory* (ed. by G. Akemann, J. Baik, P. Di Francesco) (Oxford university press, Oxford, 2011).
- [69] J. J. M. Verbaarschot, in chapter 32 of the book *The Oxford handbook of random matrix theory* (ed. by G. Akemann, J. Baik, P. Di Francesco) (Oxford university press, Oxford, 2011).
- [70] S. N. Majumdar, O. Bohigas, A. Lakshminarayan, J. Stat. Phys. **131**, 33 (2008).
- [71] P. Bianchi, M. Debbah, M. Maida, and J. Najim, IEEE T. Inform. Theory **57**, 2400 (2011).
- [72] S. N. Majumdar, G. Schehr, D. Villamaina, P. Vivo, J. Phys. A: Math. Theor. **46** 022001 (2013).
- [73] R. Allez, J.-P. Bouchaud, A. Guionnet, Phys. Rev. Lett. **109**, 094102 (2012).
- [74] R. Allez, J.-P. Bouchaud, S. N. Majumdar, P. Vivo, J. Phys. A: Math. Theor. **46**, 015001 (2013).
- [75] F. G. Tricomi, *Integral equations*, Dover publications (1985).
- [76] L. O. Chekhov, B. Eynard, O. Marchal, Theor. Math. Phys. **166**, 141 (2011).
- [77] J. Baik, R. Buckingham, J. DiFranco, Comm. Math. Phys. **280**, 463 (2008).
- [78] D. J. Gross, A. Matytsin, Nucl. Phys. B **429**, 50 (1994).
- [79] M. Marino, *Lectures on non-perturbative effects in large N gauge theories, matrix models and strings*, arXiv: 1206.6272; see also M. Marino, JHEP **0812**, 114 (2008).
- [80] L. Dumaz, B. Virág, preprint arXiv:1102.4818, to appear in Ann. Inst. H. Poincaré (2013).
- [81] G. Akemann, M. Atkin, J. Phys. A: Math. Theor. **46**, 015202 (2013).
- [82] M. Atkin, S. Zohren, arXiv: 1307.3118.
- [83] P. Vivo, S. N. Majumdar, O. Bohigas, Phys. Rev. Lett. **101**, 216809 (2008).
- [84] P. Vivo, S. N. Majumdar, O. Bohigas, Phys. Rev. B **81**, 104202 (2010).
- [85] K. Damle, S. N. Majumdar, V. Tripathi, P. Vivo, Phys. Rev. Lett. **107**, 177206 (2011).
- [86] C. Nadal, S. N. Majumdar, M. Vergassola, Phys. Rev. Lett. **104**, 110501 (2010).
- [87] C. Nadal, S. N. Majumdar, M. Vergassola, J. Stat. Phys. **142**, 403 (2011).
- [88] P. Facchi, U. Marzolino, G. Parisi, S. Pascazio, A. Scardicchio, Phys. Rev. Lett. **101**, 050502

- (2008).
- [89] A. De Pasquale, P. Facchi, G. Parisi, S. Pascazio, A. Scardicchio, Phys. Rev. A **81**, 052324 (2010).
 - [90] P. Katakopoulos, P. Mertikopoulos, A. L. Moustakas, G. Caire, IEEE T. Inform. Theory **57**, 1984 (2011).
 - [91] F. Colomo, A. G. Pronko, arXiv:1306.6207, to appear in Phys. Rev. E.
 - [92] C. Tracy, H. Widom, Ann. Appl. Probab. **17**, 953 (2007).
 - [93] N. Bonichon, M. Mosbah, Theor. Comput. Sci. **307**, 241 (2003).
 - [94] G. Schehr, S. N. Majumdar, A. Comtet, J. Randon-Furling, Phys. Rev. Lett. **101**, 150601 (2008).
 - [95] M. Katori, M. Izumi, N. Kobayashi, J. Stat. Phys. **131**, 1067 (2008).
 - [96] N. Kobayashi, M. Izumi, M. Katori, Phys. Rev. E **78**, 051102 (2008).
 - [97] T. Feierl, J. Phys. A: Math. Theor. **45**, 095003 (2012).
 - [98] J. Rambeau, G. Schehr, Europhys. Lett. **91**, 60006 (2010).
 - [99] J. Rambeau, G. Schehr, Phys. Rev. E **83**, 061146 (2011).
 - [100] A. Borodin, P. L. Ferrari, M. Praehofer, T. Sasamoto, J. Warren, Electron. Comm. Probab. **14**, 486 (2009).
 - [101] M. Crescimanno, S. G. Naculich, H. J. Schnitzer, Phys. Rev. D **54**, 1809 (1996).
 - [102] C. W. J. Beenakker, Rev. Mod. Phys. **69**, 731 (1997).
 - [103] R. Landauer, IBM J. Res. Dev. **1**, 223 (1957); Phil. Mag. **21**, 863 (1970).
 - [104] Ya. M. Blanter, M. Büttiker, Phys. Rep. **336**, 1 (2000).
 - [105] H.-J. Sommers, W. Wicczorek, D. Savin, Acta Phys. Pol. A **112**, 691 (2007).
 - [106] B. A. Khoruzenko, D.V. Savin, H.-J. Sommers, Phys. Rev. B **80**, 125301 (2009).
 - [107] V. Al. Osipov, E. Kanzieper, Phys. Rev. Lett. **101**, 216809 (2008).
 - [108] D. N. Page, Phys. Rev. Lett. **71**, 1291 (1993).
 - [109] V. Periwal, D. Shevitz, Phys. Rev. Lett. **64**, 1326 (1990).
 - [110] E. Brézin, C. Itzykson, G. Parisi, J. B. Zuber, Comm. Math. Phys. **59**, 35 (1978).
 - [111] T. Claeys, A. Its, I. Krasovsky, Comm. Pure Appl. Math. **63**, 362 (2010).
 - [112] T. Claeys, S. Olver, in *Recent Advances in Orthogonal Polynomials, Special Functions, and Their Applications*, Contemporary Mathematics 578, Amer. Math. Soc., Providence R.I, 83 (2012).
 - [113] S. N. Majumdar, C. Nadal, A. Scardicchio, P. Vivo, Phys. Rev. Lett. **103**, 220603 (2009).
 - [114] S. N. Majumdar, C. Nadal, A. Scardicchio, P. Vivo, Phys. Rev. E **83**, 041105 (2011).
 - [115] S. N. Majumdar, P. Vivo, Phys. Rev. Lett. **108**, 200601 (2012).
 - [116] C. Texier, S. N. Majumdar, Phys. Rev. Lett. **110**, 250602 (2013).
 - [117] R. Allez, J. Touboul, G. Wainrib, arXiv:1310.5039.